

Title: Superconducting accelerometer technology for precision tests of gravitation and search for new interactions

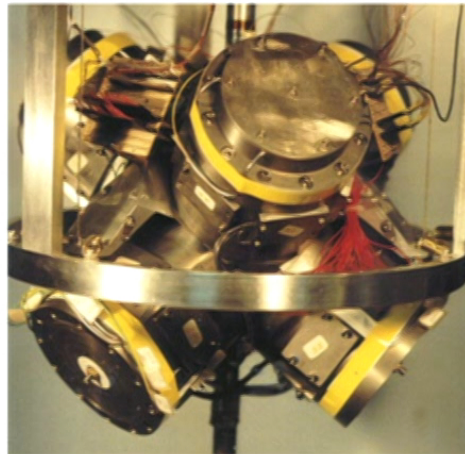
Date: Aug 21, 2017 04:00 PM

URL: <http://pirsa.org/17080021>

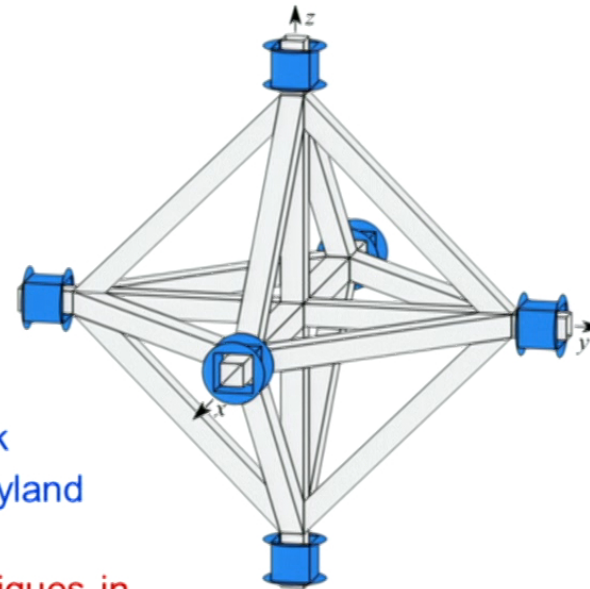
Abstract:



Superconducting Accelerometer Technology for Precision Tests of Gravitation and Search for New Interactions



Ho Jung Paik
University of Maryland



Experimental Techniques in
Table-top Fundamental Physics
Waterloo, August 21-25, 2017



Birth of s/c accelerometer



Development of cryogenic GW detector at Stanford (1970)

Motion of 5 ton antenna must be detected to $< 10^{-20} \text{ m Hz}^{-1/2}$.

Paik-2



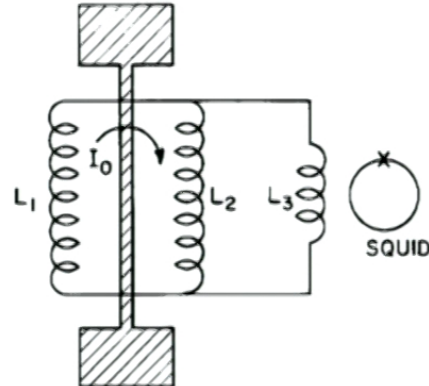
Birth of s/c accelerometer



Development of cryogenic GW detector at Stanford (1970)

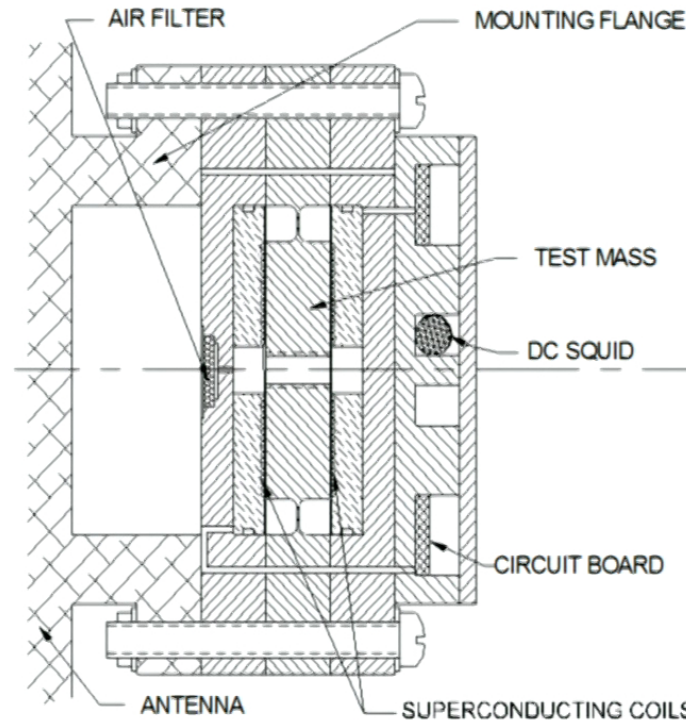
Motion of 5 ton antenna must be detected to $< 10^{-20} \text{ m Hz}^{-1/2}$.

S/C resonant transducer (1972)



$$\omega_0^2 = \omega_m^2 + \frac{2}{1+\gamma} \frac{B^2 A}{\mu_0 m d}, \quad \gamma \equiv \frac{L_3}{L_p}$$

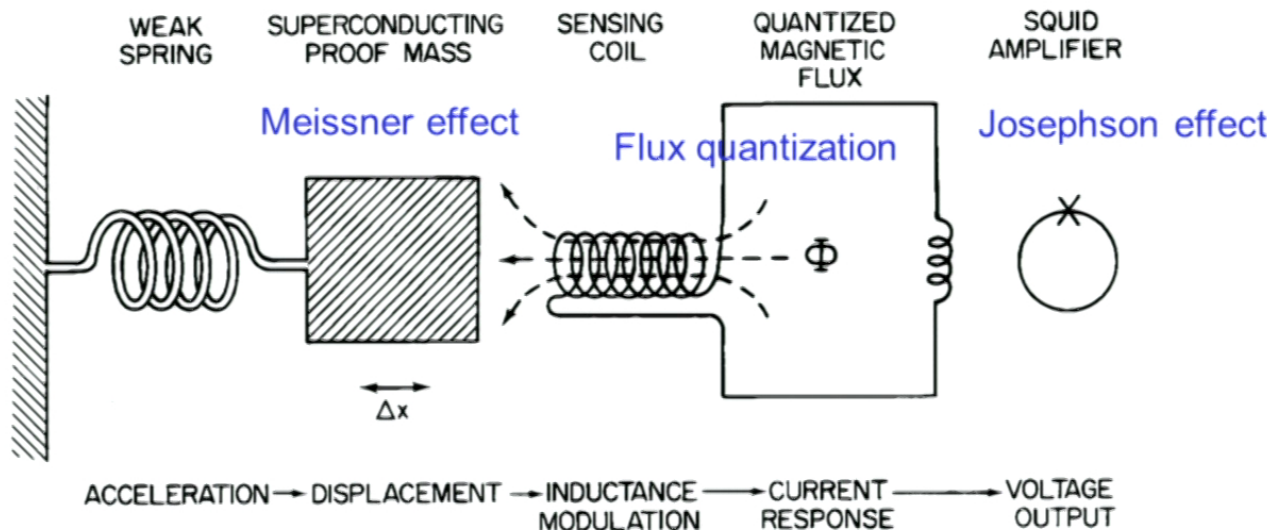
$$\beta = 1 - \left(\frac{\omega_m}{\omega_0} \right)^2 = \frac{2}{1+\gamma} \frac{B^2 A}{\mu_0 m \omega_0^2 d} \approx \frac{1}{2}$$



Paik-2



Superconducting accelerometer

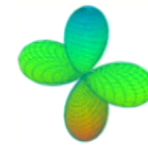


- Low noise:
 - Extremely stable scale factors \Rightarrow Sensitive differential measurement possible.
- $$S_a(f) = \frac{4}{m} \left[k_B T \frac{\omega_0}{Q} + \frac{\omega_0^2}{2\beta\eta} E_A(f) \right]$$

Paik-3



Gravity gradients



- To measure gravity field on **two or more** masses must be **differenced**.
- Gravity gradient Γ_{ij} is a symmetric 3×3 tensor:

$$\Gamma_{ij} = -\frac{\partial^2 \phi}{\partial x_i \partial x_j} = \begin{pmatrix} \Gamma_{11} & \Gamma_{12} & \Gamma_{13} \\ \Gamma_{12} & \Gamma_{22} & \Gamma_{23} \\ \Gamma_{13} & \Gamma_{23} & \Gamma_{33} \end{pmatrix}. \quad \Gamma_{11} + \Gamma_{22} + \Gamma_{33} = -\nabla^2 \phi = 0$$

⇒ 5 independent components



Gravity gradients

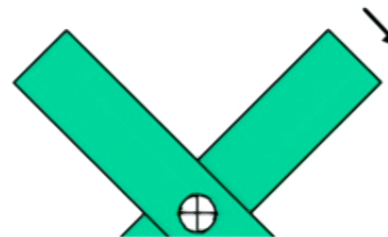
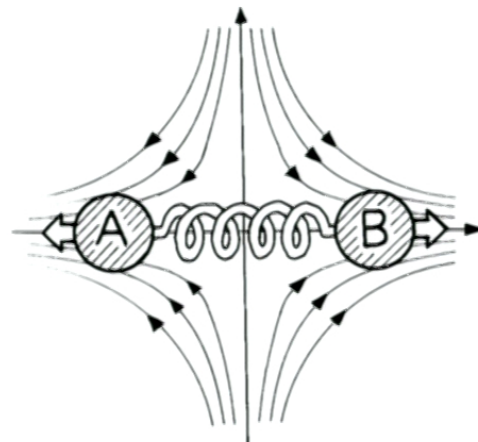


- To measure gravity field on **two or more** masses must be **differenced**.
- Gravity gradient Γ_{ij} is a symmetric 3×3 tensor:

$$\Gamma_{ij} = -\frac{\partial^2 \phi}{\partial x_i \partial x_j} = \begin{pmatrix} \Gamma_{11} & \Gamma_{12} & \Gamma_{13} \\ \Gamma_{12} & \Gamma_{22} & \Gamma_{23} \\ \Gamma_{13} & \Gamma_{23} & \Gamma_{33} \end{pmatrix}. \quad \Gamma_{11} + \Gamma_{22} + \Gamma_{33} = -\nabla^2 \phi = 0$$

⇒ 5 independent components

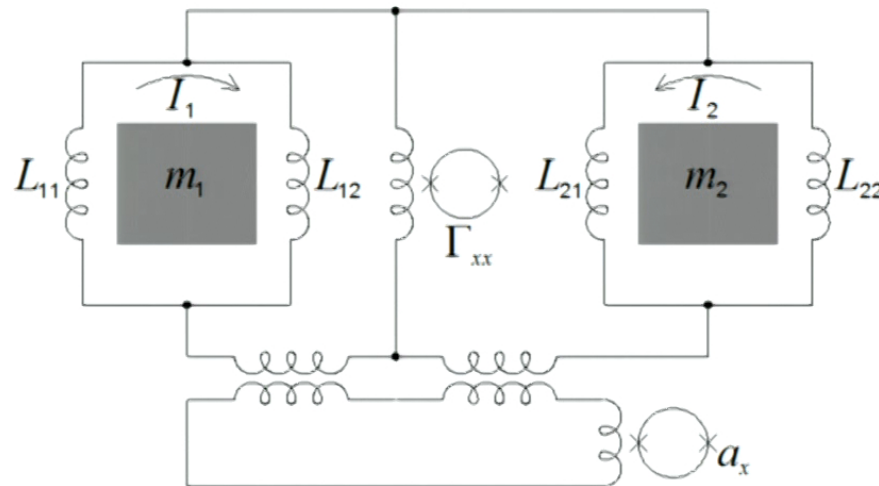
Γ_{ii} : “in-line-component” $\Gamma_{ij} (j \neq i)$: “cross-component”



Paik-4



Superconducting gravity gradiometer

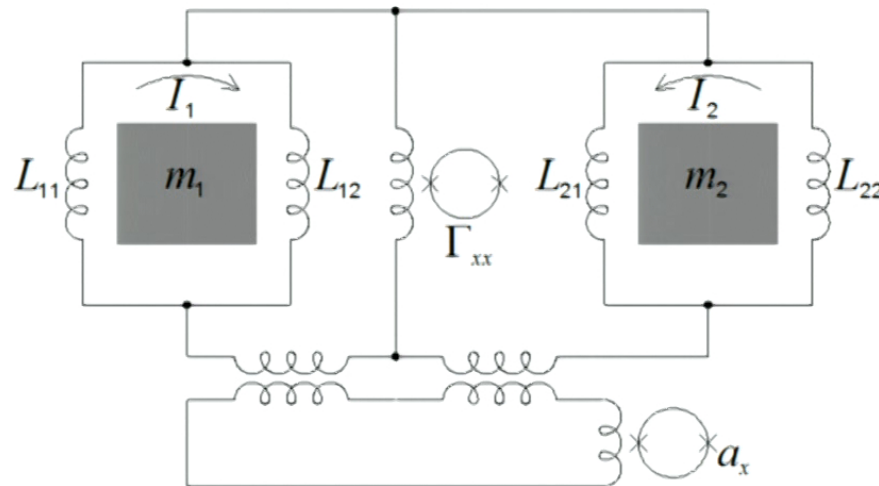
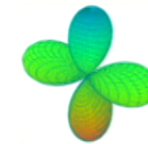


- Low noise:
$$S_{\Gamma}(f) = \frac{8}{m\ell^2} \left[k_B T \frac{\omega_D}{Q} + \frac{\omega_D^2}{2\beta\eta} E_A(f) \right]$$
$$S_{\Gamma}^{1/2}(f) \approx 2 \times 10^{-3} \text{ E Hz}^{-1/2}, 1 \text{ E} \equiv 10^{-9} \text{ s}^{-2} (\Gamma_{zz, \text{Earth}} \approx 3 \times 10^3 \text{ E})$$
- I_2/I_1 are adjusted to balance out CM. \Rightarrow Stable CM rejection $> 10^7$.

Paik-5



Superconducting gravity gradiometer

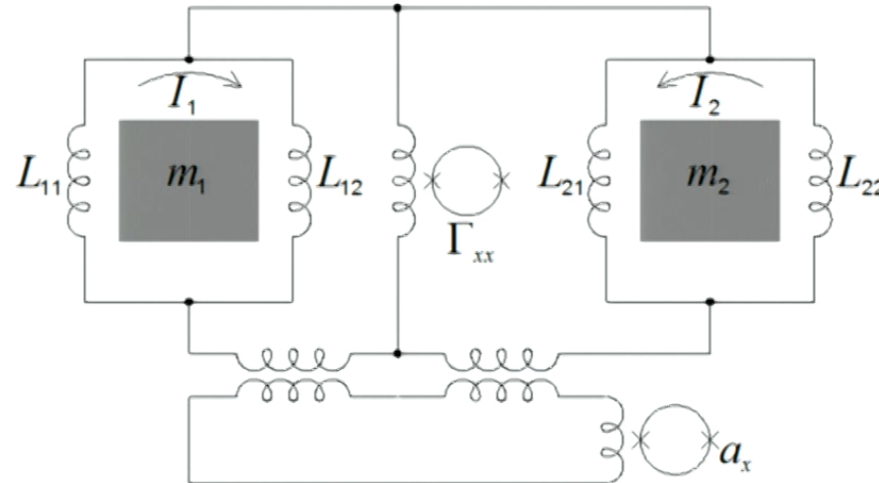


- Low noise:
$$S_{\Gamma}(f) = \frac{8}{m\ell^2} \left[k_B T \frac{\omega_D}{Q} + \frac{\omega_D^2}{2\beta\eta} E_A(f) \right]$$
$$S_{\Gamma}^{1/2}(f) \approx 2 \times 10^{-3} \text{ E Hz}^{-1/2}, 1 \text{ E} \equiv 10^{-9} \text{ s}^{-2} (\Gamma_{zz, \text{Earth}} \approx 3 \times 10^3 \text{ E})$$
- I_2/I_1 are adjusted to balance out CM. \Rightarrow Stable CM rejection $> 10^7$.

Paik-5



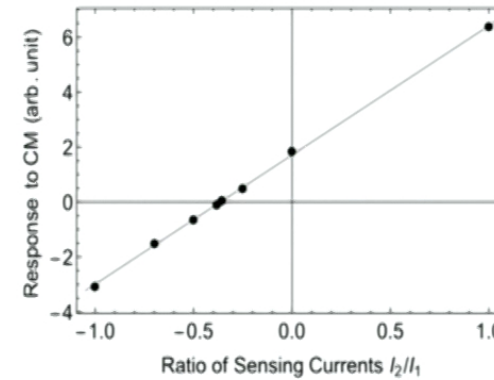
Superconducting gravity gradiometer



- Low noise:
$$S_\Gamma(f) = \frac{8}{m\ell^2} \left[k_B T \frac{\omega_D}{Q} + \frac{\omega_D^2}{2\beta\eta} E_A(f) \right]$$

$$S_{\Gamma}^{1/2}(f) \approx 2 \times 10^{-3} \text{ E Hz}^{-1/2}, 1 \text{ E} \equiv 10^{-9} \text{ s}^{-2} (\Gamma_{zz, \text{Earth}} \approx 3 \times 10^3 \text{ E})$$

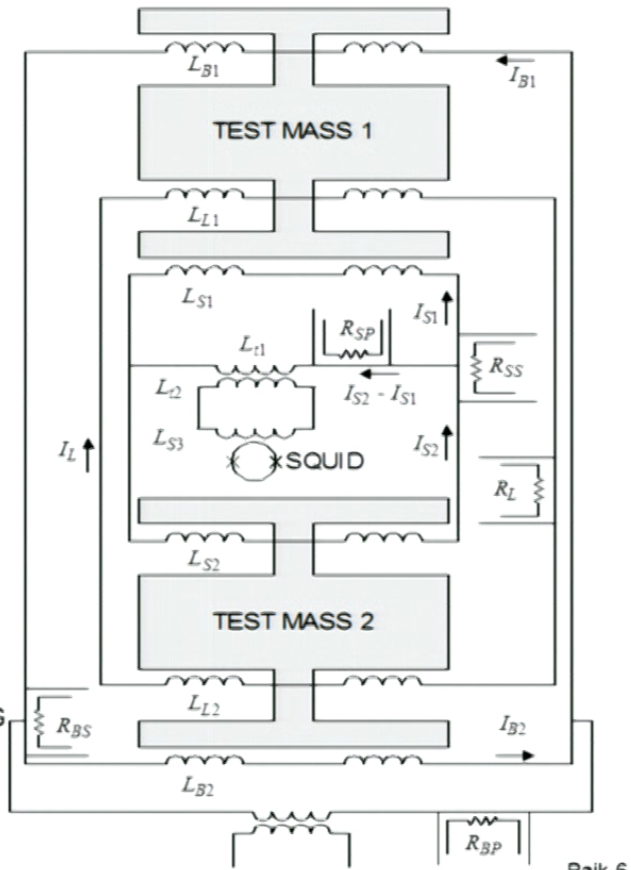
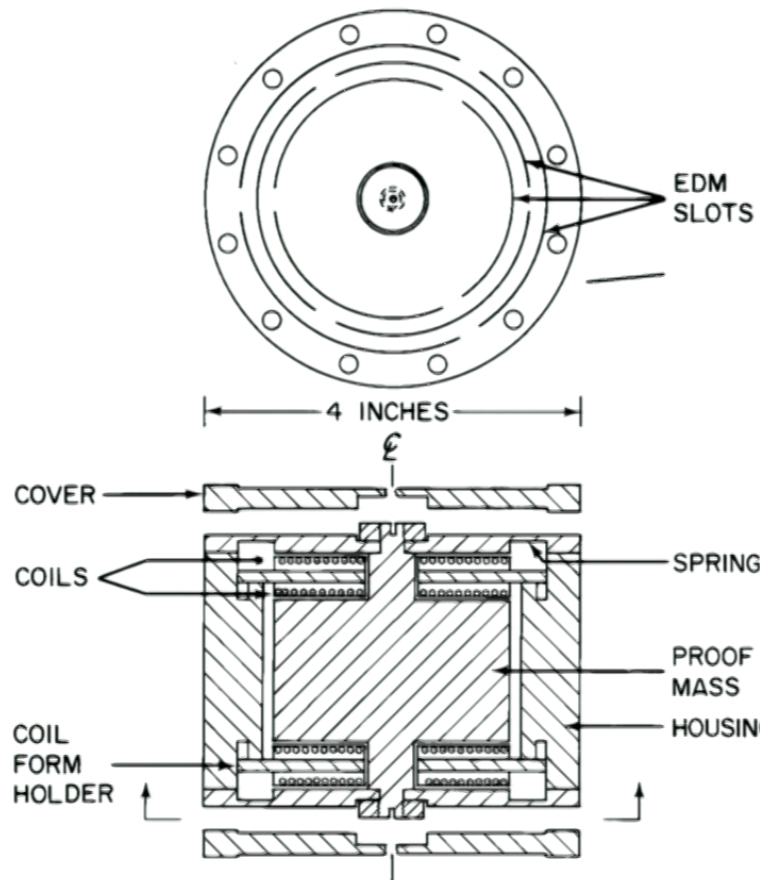
- I_2/I_1 are adjusted to balance out CM. \Rightarrow Stable CM rejection $> 10^7$.



Paik-5



Model II SGG



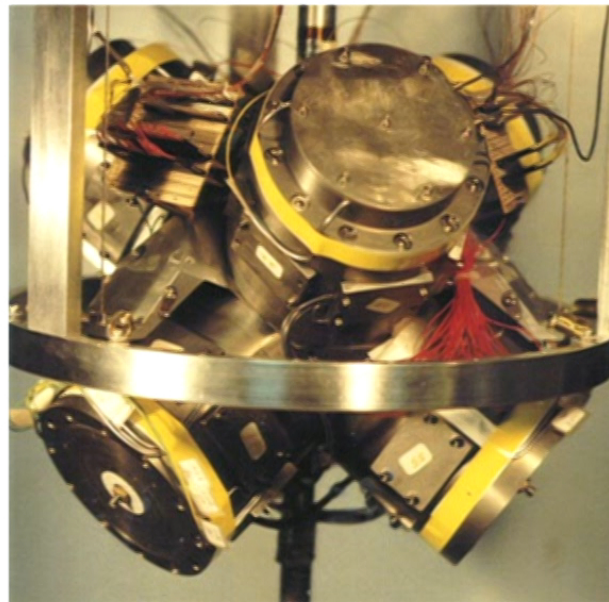
Paik-6



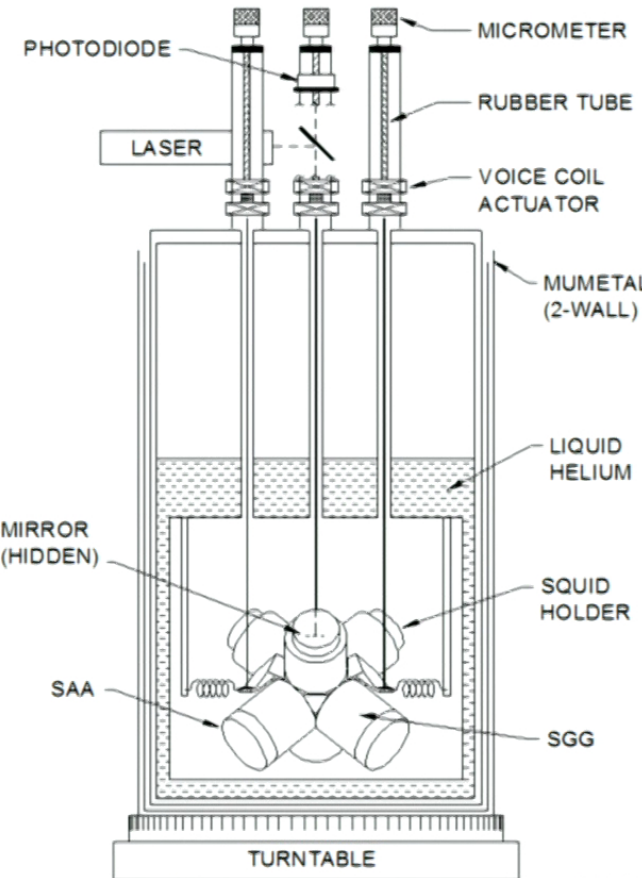
SGG in the cryostat



3-axis with mechanical suspension



Moody et al, RSI 73, 3957 (2002)



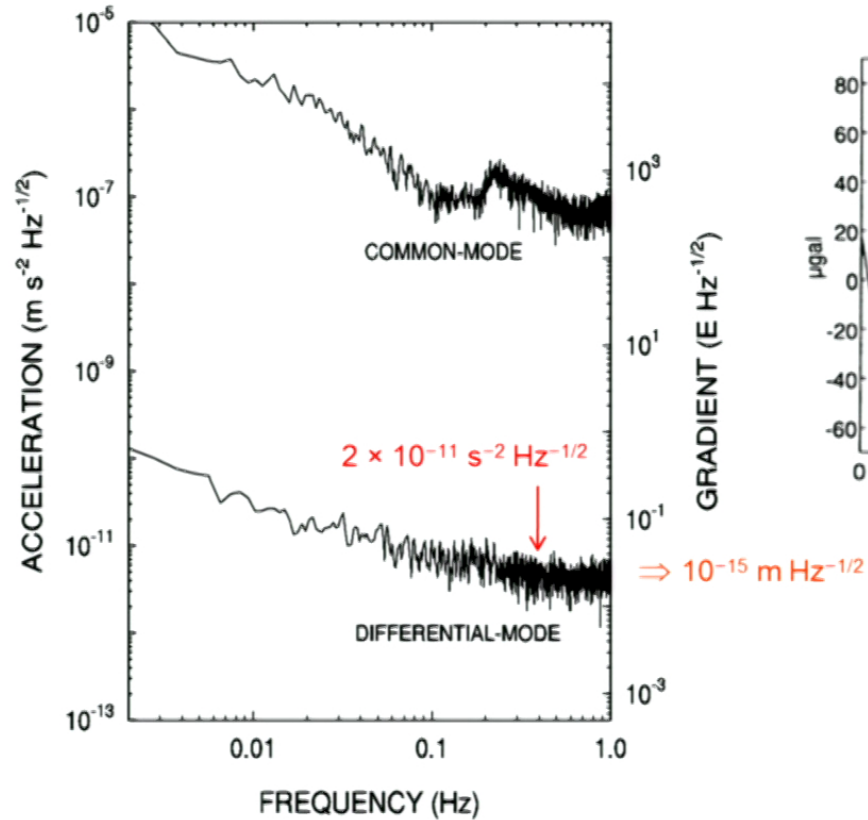
Paik-7



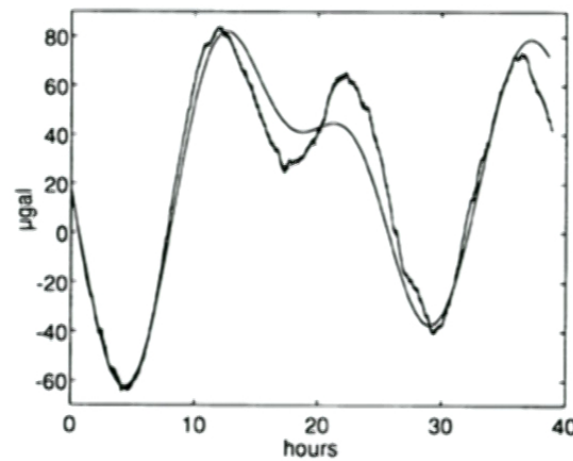
Performance of Model II SGG



Gravity gradient noise PSD



Gravimeter Mode



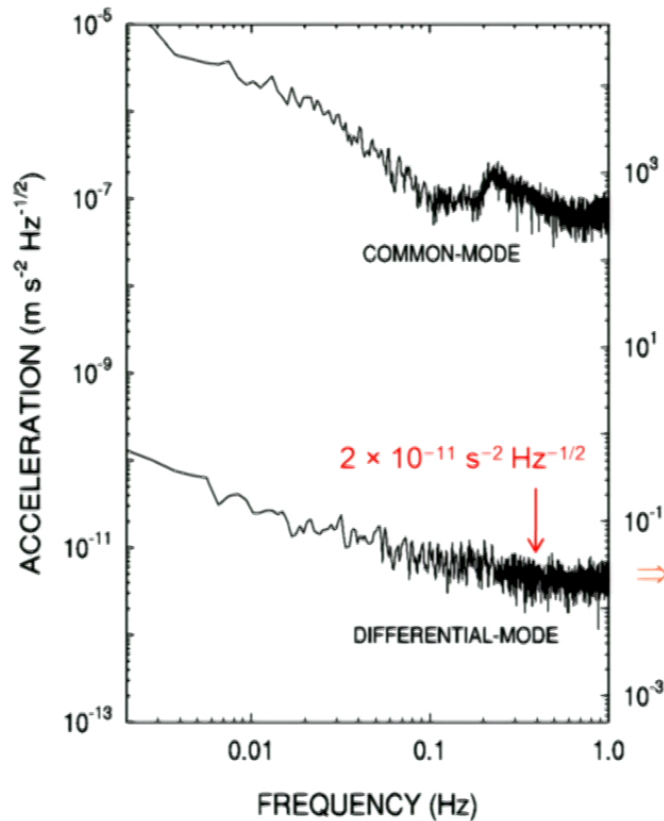
Paik-8



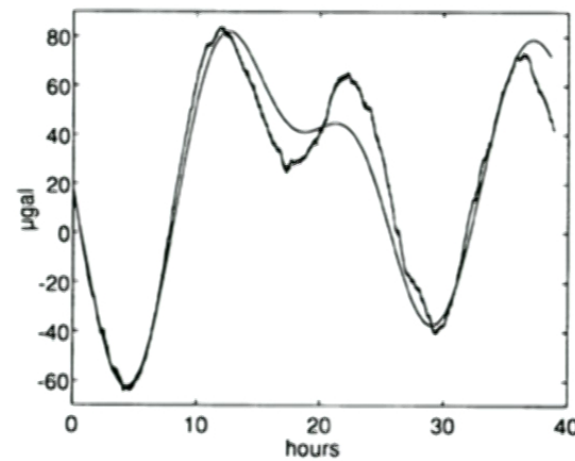
Performance of Model II SGG



Gravity gradient noise PSD



Gravimeter Mode

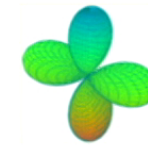


By early 1990's, SGG achieved sensitivity 10^3 times better than any other gradiometers to date.

Paik-8



Gauss's law test of the $1/r^2$ law



- Motivation: Many modern theories of gravity predict

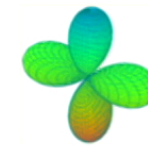
$$\phi(r) = -\frac{GM}{r} \left[1 + \alpha e^{-r/R} \right]$$

Fifth force?

Paik-10



Gauss's law test of the $1/r^2$ law



- Motivation: Many modern theories of gravity predict

$$\phi(r) = -\frac{GM}{r} \left[1 + \alpha e^{-r/R} \right]$$

Fifth force?

Paik-10

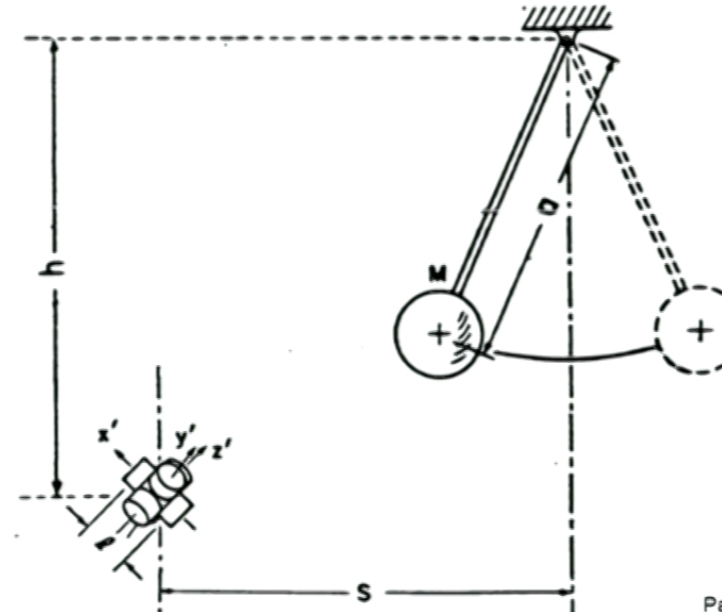


Gauss's law test of the $1/r^2$ law



- Motivation: Many modern theories of gravity predict $\phi(r) = -\frac{GM}{r} [1 + \alpha e^{-r/R}]$
Fifth force?
- Principle: Newton's law is equivalent to Gauss's law: $\nabla \cdot \mathbf{g} = -\nabla^2 \phi = -4\pi G\rho$
- Source mass: 1.5-ton lead (Pb) pendulum
- Detector: 3-axis SGG

$$\nabla \cdot \mathbf{g} = 0 ?$$

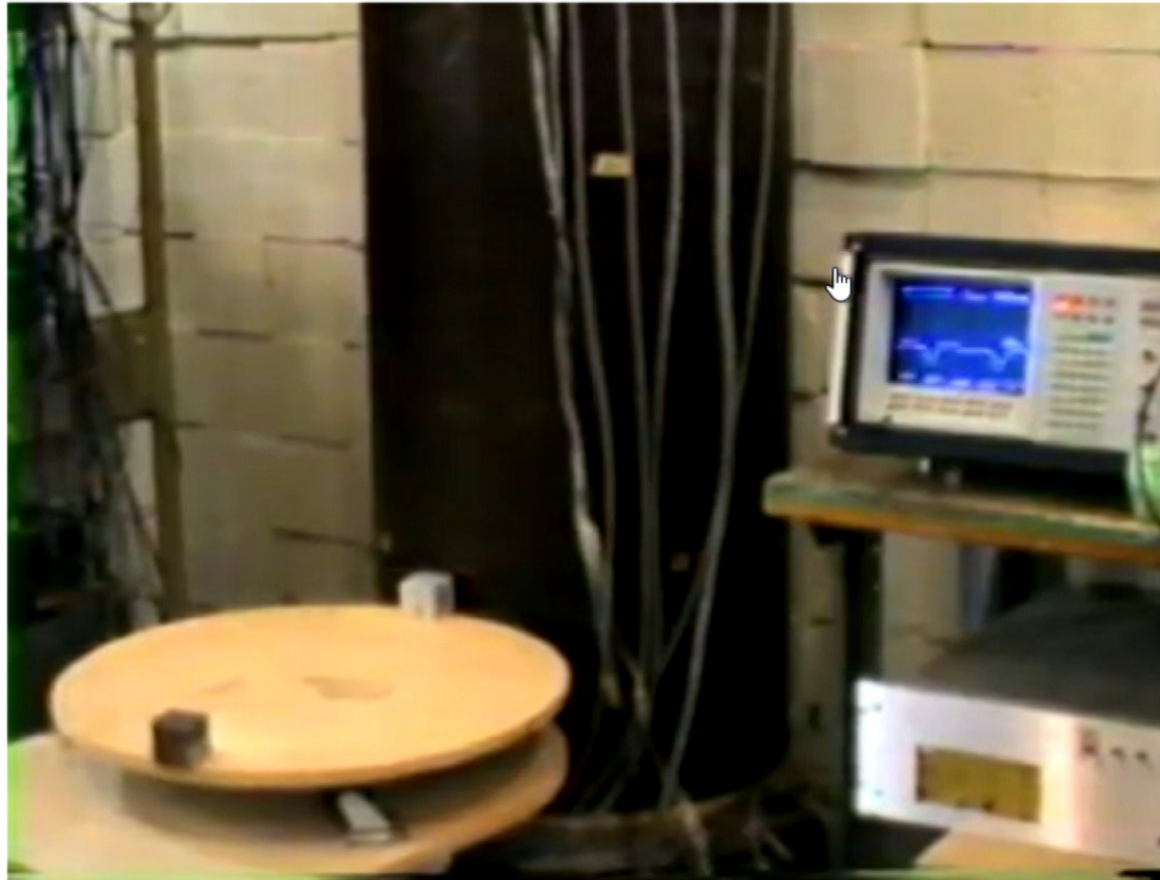


Paik-10



Demonstration of Model 2 SGG

www.physics.umd.edu/GRE/SGG_video.htm



Paik-9





Demonstration of Model 2 SGG

www.physics.umd.edu/GRE/SGG_video.htm

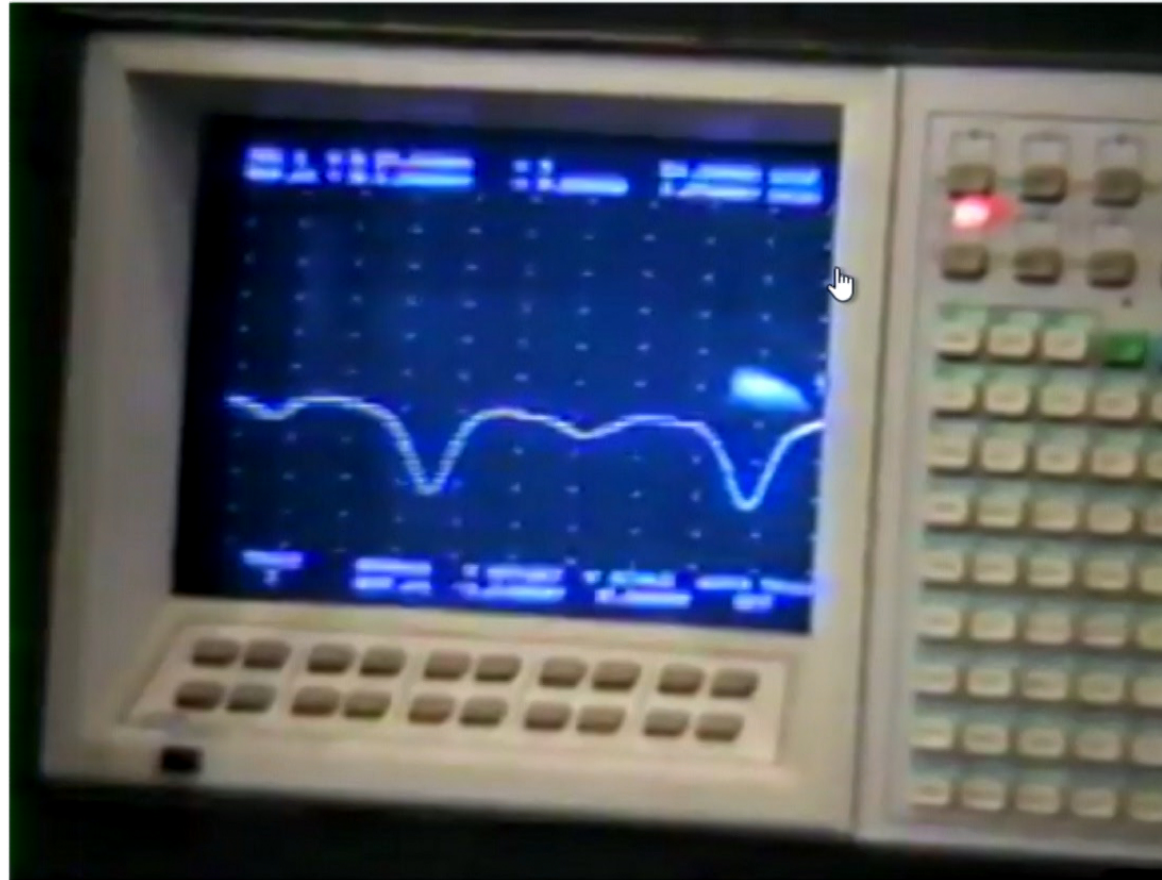


Paik-9



Demonstration of Model 2 SGG

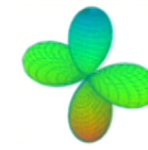
www.physics.umd.edu/GRE/SGG_video.htm



Paik-9



Gauss's law test of the $1/r^2$ law



- Motivation: Many modern theories of gravity predict

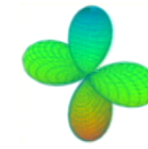
$$\phi(r) = -\frac{GM}{r} \left[1 + \alpha e^{-r/R} \right]$$

Fifth force?

Paik-10

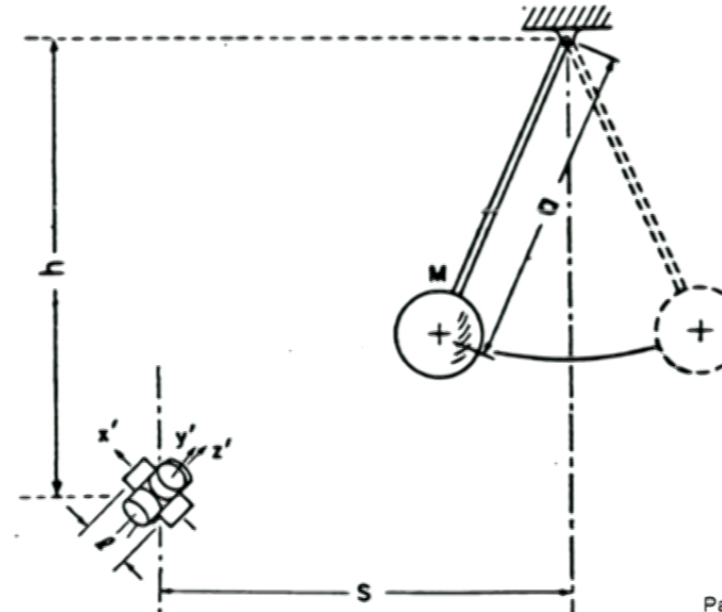


Gauss's law test of the $1/r^2$ law



- Motivation: Many modern theories of gravity predict $\phi(r) = -\frac{GM}{r} [1 + \alpha e^{-r/R}]$
Fifth force?
- Principle: Newton's law is equivalent to Gauss's law: $\nabla \cdot \mathbf{g} = -\nabla^2 \phi = -4\pi G\rho$
- Source mass: 1.5-ton lead (Pb) pendulum
- Detector: 3-axis SGG

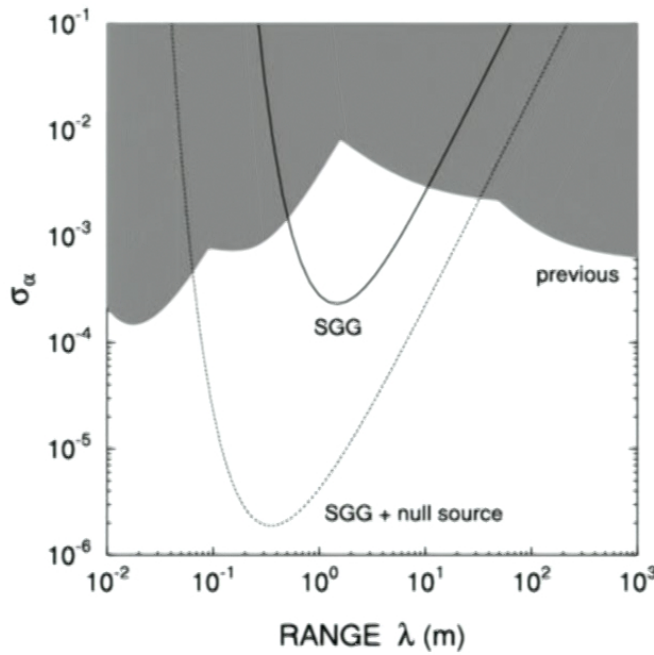
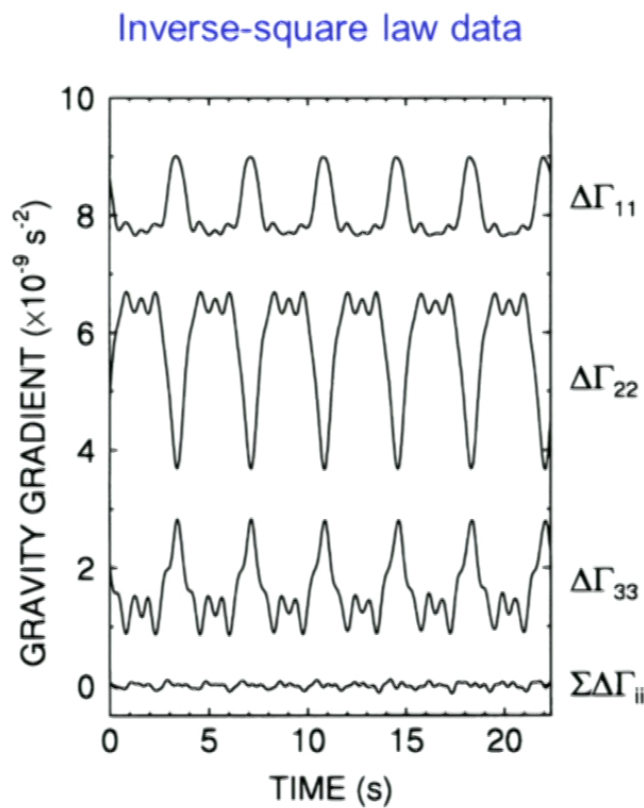
$$\nabla \cdot \mathbf{g} = 0 ?$$



Paik-10



Experimental result



$$\alpha = (0.9 \pm 4.6) \times 10^{-4} \text{ at } \lambda = 1.5 \text{ m}$$

Moody & Paik, *PRL* 70, 1195 (1993)

Paik-11



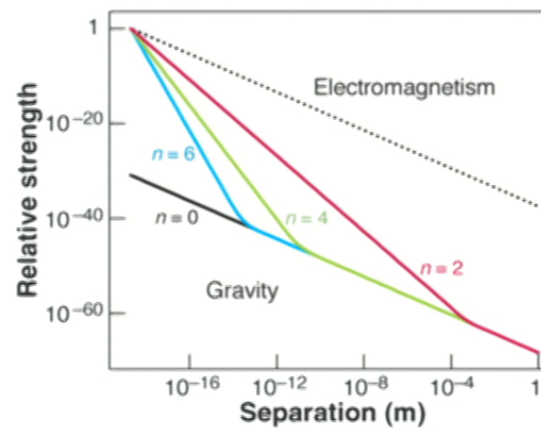
Gravity-only extra dimensions?

Input: DVI - 1920x1080p@60Hz
Output: SDI - 1920x1080i@60Hz



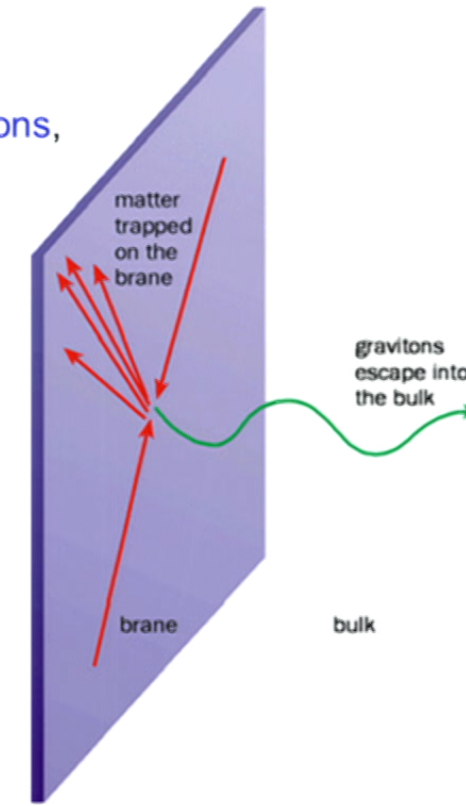
Hierarchy problem in the field theory

- Why is gravity 10^{40} times weaker than EM?
- Gravity may escape into n gravity-only extra dimensions, (Arkani-Hamed, Dimopoulos and Dvali, 1998).



- For $r > R$,
$$\phi(r) = -\frac{GM}{r} \left[1 + \alpha e^{-r/R} \right]$$

 \Rightarrow For two large dimensions of similar size,
 $\alpha = 4$, $R_1 \approx R_2 \approx 1 \text{ mm}$ (Arkani-Hamed et al., 1999).



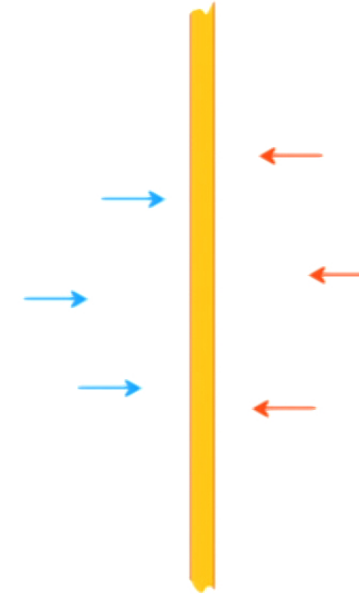
Paik-12



UM experiment



- Principle: $\nabla \phi_N$ is constant in position on either side of an **infinite plane slab**.
- Source: **Ta** ($\rho = 16.6 \text{ g cm}^{-3}$) disk of large diameter-to-thickness (**null source**).
- Detector: Differential accelerometer formed by two thin **Nb** disks, located at $\sim 200 \mu\text{m}$ from source.
⇒ **Seismic noise rejected** by CMRR = 10^3 .



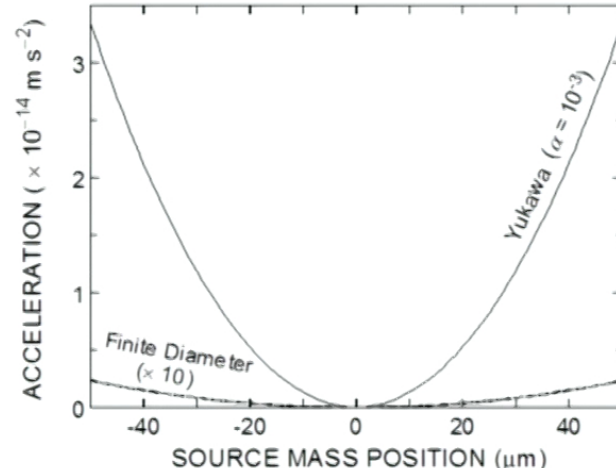
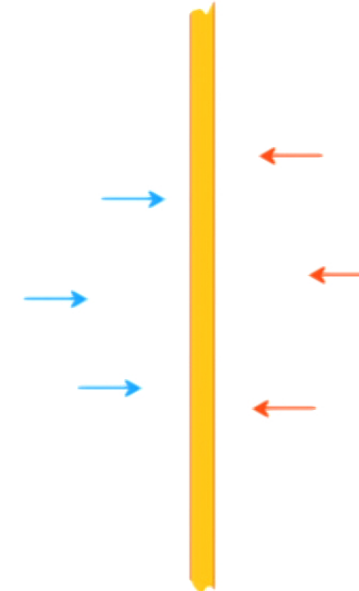
Paik-13



UM experiment



- Principle: $\nabla \phi_N$ is constant in position on either side of an **infinite plane slab**.
- Source: **Ta** ($\rho = 16.6 \text{ g cm}^{-3}$) disk of large diameter-to-thickness (**null source**).
- Detector: Differential accelerometer formed by two thin **Nb** disks, located at $\sim 200 \mu\text{m}$ from source.
⇒ **Seismic noise rejected** by $\text{CMRR} = 10^3$.

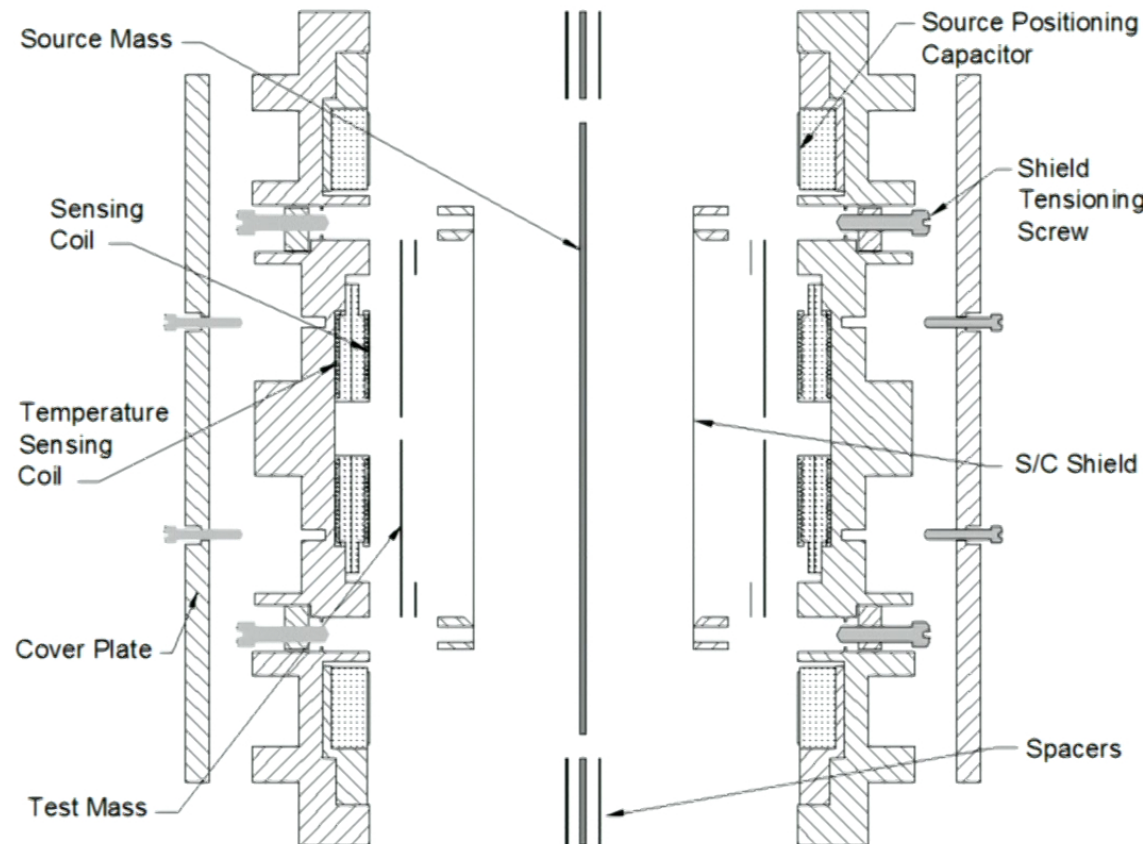


As the source is driven at f , the differential signal appears at $2f$.
⇒ **This reduces mechanical and magnetic cross-talk.**

Paik-13



Exploded view of the experiment



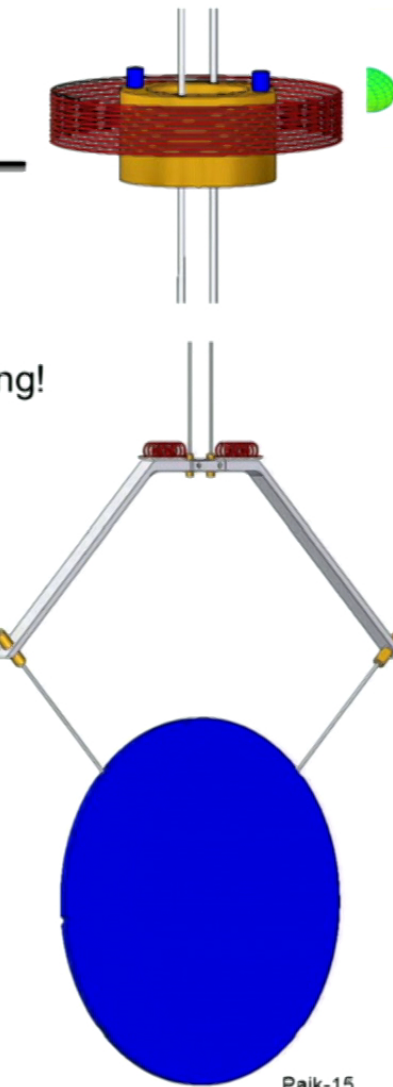
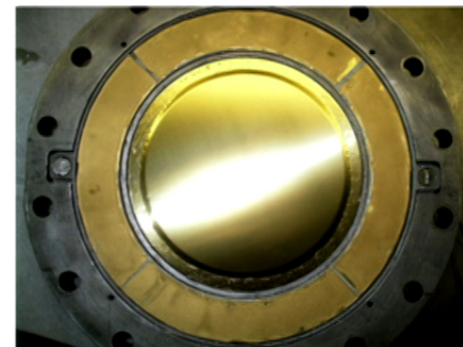
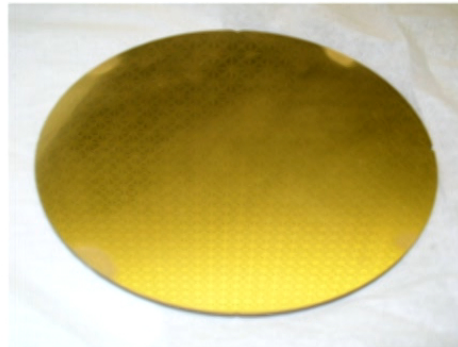
Paik-14



Apparatus

- To decouple source motion from the detector and make it purely sinusoidal, the source **is driven from the top of the cryostat**.
- Disadvantage: source-detector **alignment** is very challenging!
- To reduce the patch field potential, the mating source and detector surfaces are **coated with gold**.

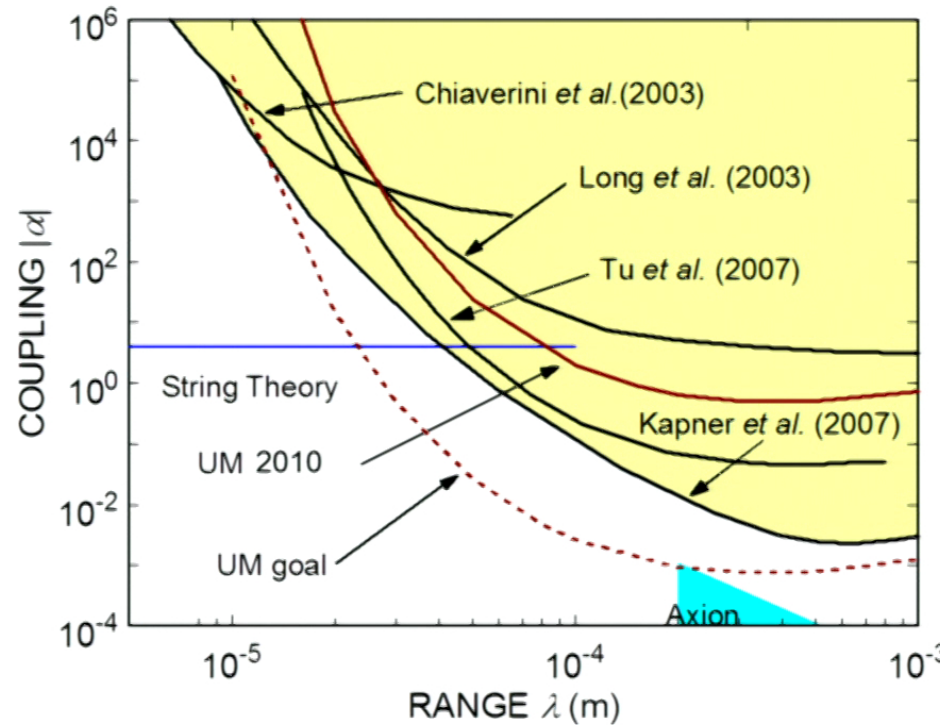
$$F_p(d) = -\frac{\epsilon_0 v^2}{2d^2}, \quad v_{Nb} \approx 1 \text{ V}, \quad v_{Au} \approx 0.16 \text{ V}$$



Paik-15



Experimental result



$$\alpha = 0.9 \pm 1.0 \text{ at } \lambda = 100 \mu\text{m}$$

No extra dimensions were found (95% CL) down to $\lambda = 78 \mu\text{m}$.

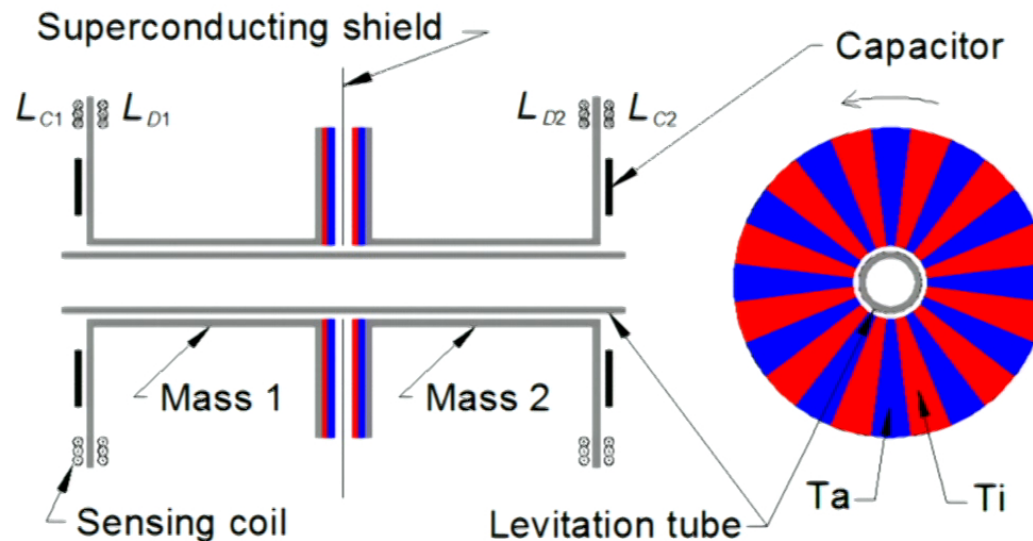
Paik-16



UM2 with density-modulated source



- $1/r^2$ law test using a **distance-modulated** source becomes increasingly difficult as λ decreases because the source modulates parasitic forces from patch fields, Casimir effect, and residual pressure.
- By using a **density-modulated** source moving laterally, it may be possible to extend the search for extra dimensions to $\lambda \sim 10 \mu\text{m}$.



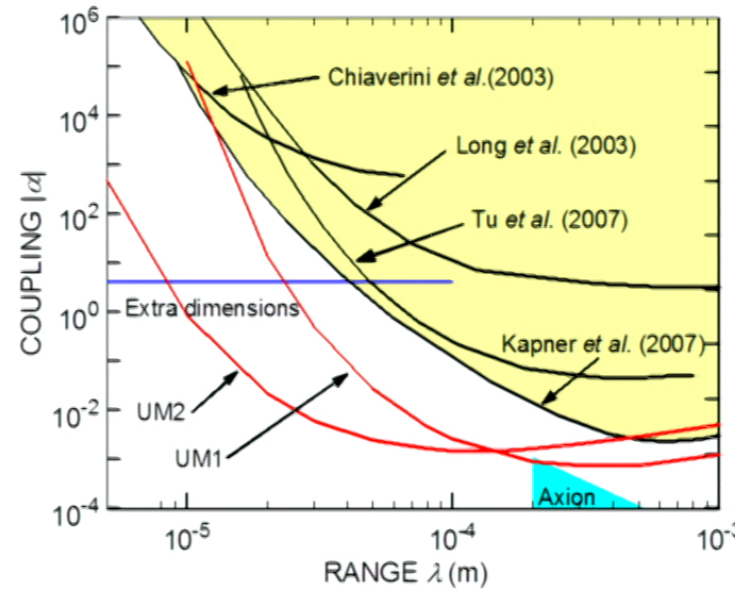
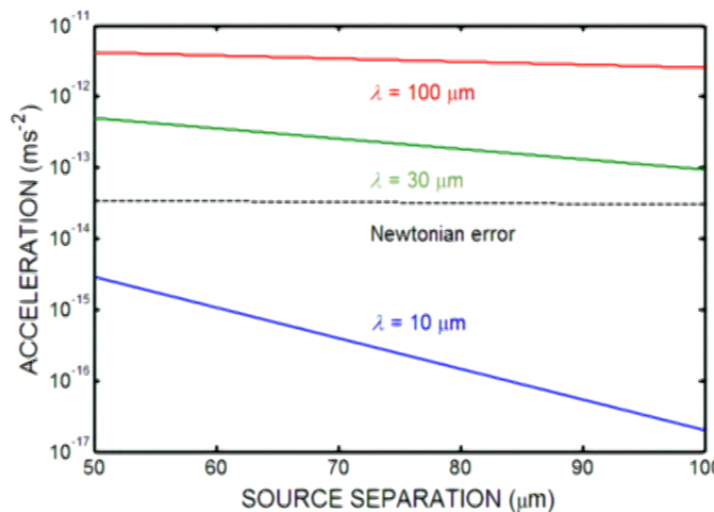
Paik-17



Potential sensitivity of UM2



- Yukawa signal is sensitive to separation d , especially for $\lambda \leq 30 \mu\text{m}$, whereas **Newtonian signal** varies by **only 2%** as d varies from 50 to 100 μm .
- By repeating test at $d = 50$ and 100 μm and subtracting the two results, 98% of **metrology error** is removed while Yukawa signal remains almost unchanged.



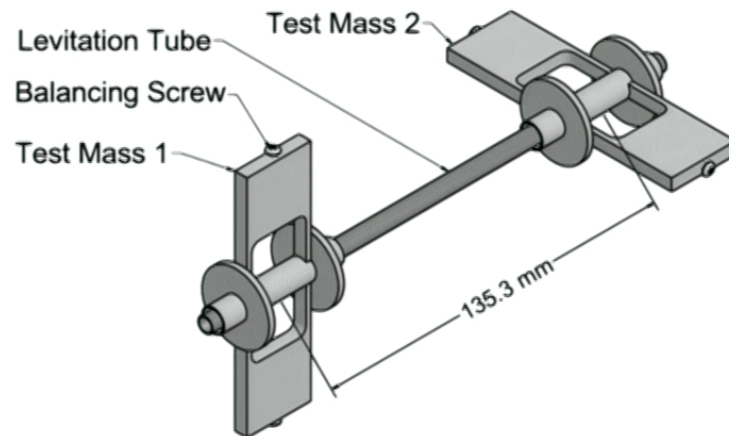
Paik-19



SGG with levitated masses



- New levitated SGG is under development with NASA support.
- A pair of test masses with orthogonal moment arms are levitated by a current on a [single levitation tube](#).



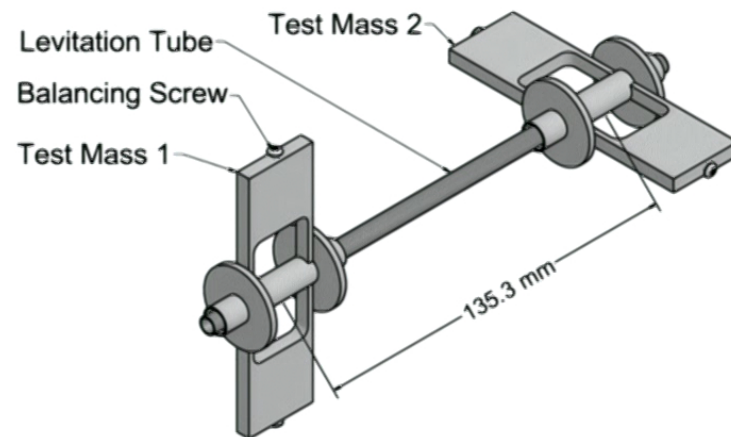
Paik-20



SGG with levitated masses



- New levitated SGG is under development with NASA support.
- A pair of test masses with orthogonal moment arms are levitated by a current on a [single levitation tube](#).



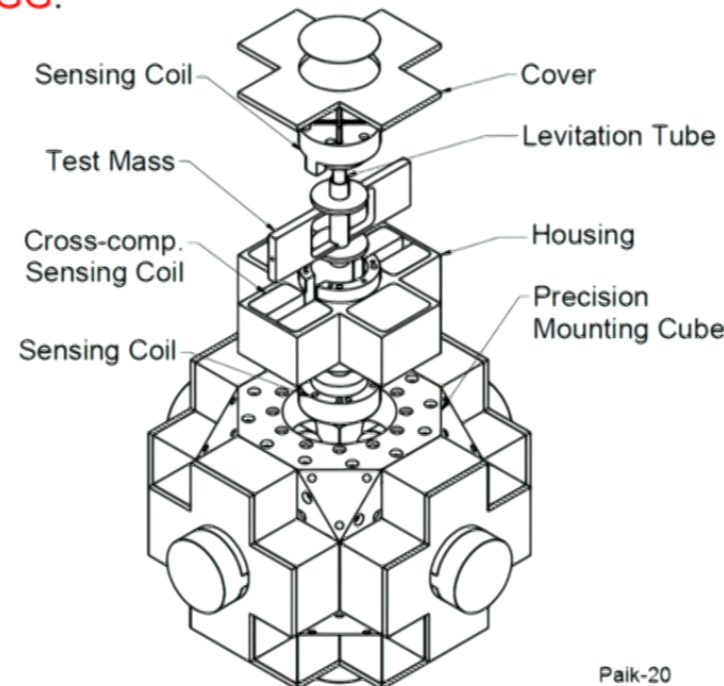
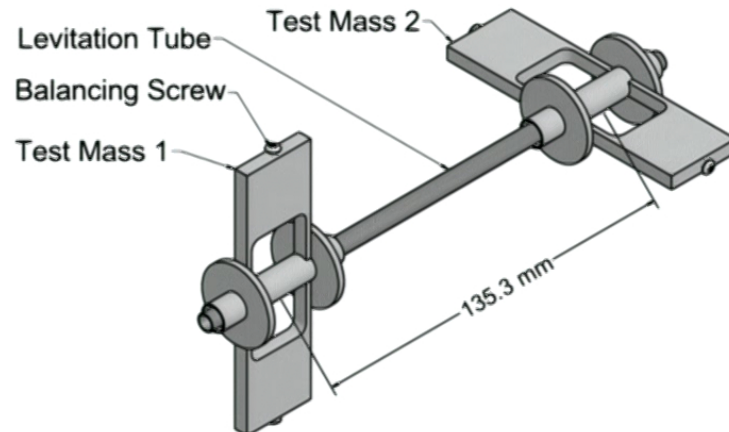
Paik-20



SGG with levitated masses

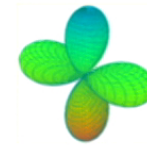


- New levitated SGG is under development with NASA support.
- A pair of test masses with orthogonal moment arms are levitated by a current on a [single levitation tube](#).
- **Three** orthogonal pairs form a **tensor SGG**.

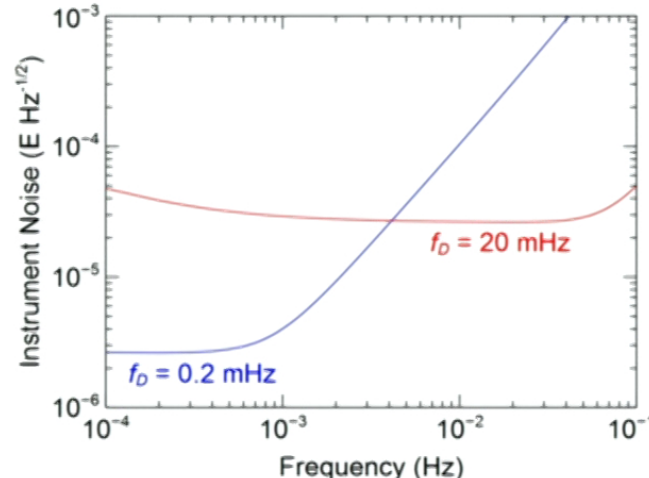




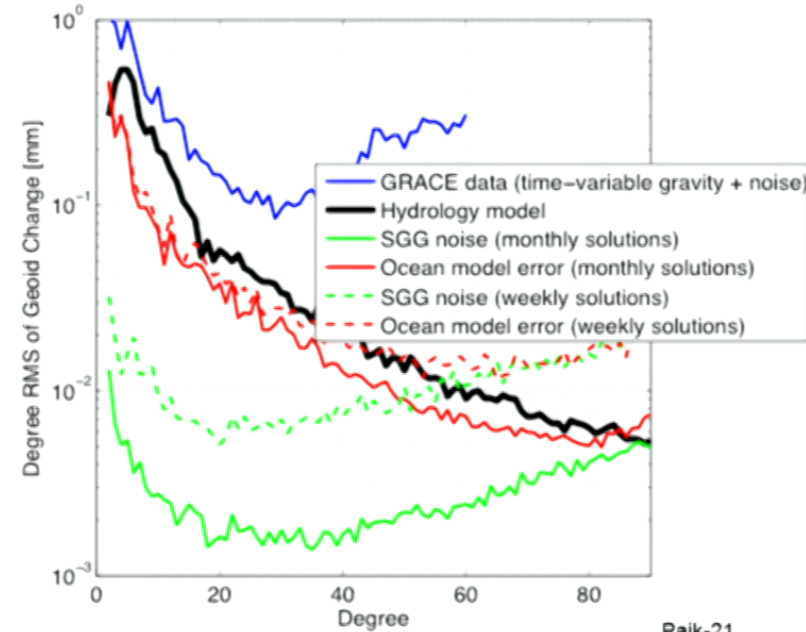
SGG Earth science mission



- Tensor SGG with $m = 1 \text{ kg}$, $\ell = 0.2 \text{ m}$, $S_{\Gamma}^{1/2}(f) = 3 \times 10^{-5} \text{ E Hz}^{-1/2}$ over $0.5 \sim 50 \text{ mHz}$.
- SGG could be *tuned* during the mission to yield **higher sensitivity at high f** for high spatial resolution **or low f** for time-variable gravity signals.
- Cryocooler will permit **5-10 year** mission lifetime.



Instrument noise spectral density



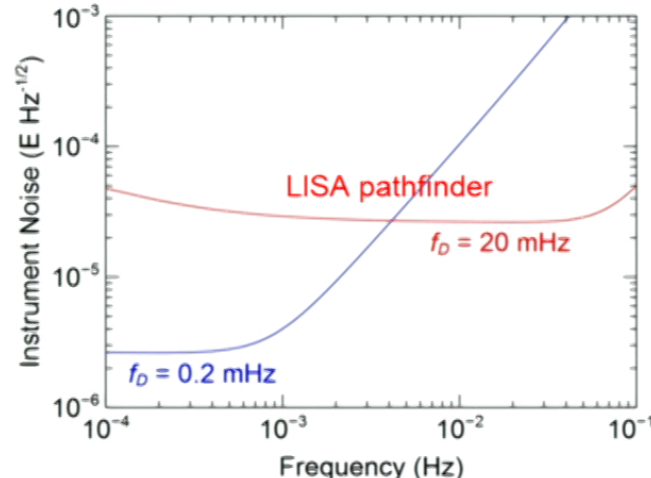
Paik-21



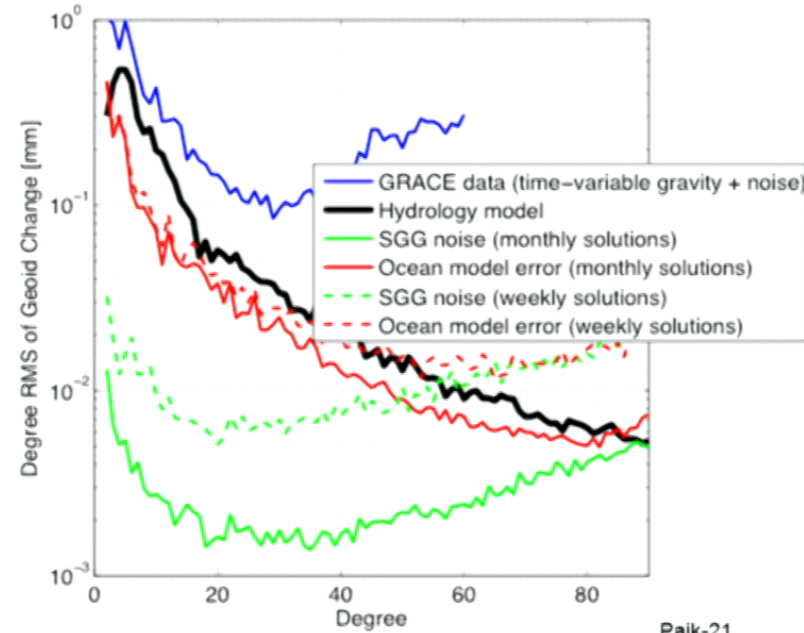
SGG Earth science mission



- Tensor SGG with $m = 1 \text{ kg}$, $\ell = 0.2 \text{ m}$, $S_{\Gamma}^{1/2}(f) = 3 \times 10^{-5} \text{ E Hz}^{-1/2}$ over $0.5 \sim 50 \text{ mHz}$.
- SGG could be *tuned* during the mission to yield **higher sensitivity at high f** for high spatial resolution **or low f** for time-variable gravity signals.
- Cryocooler will permit **5-10 year** mission lifetime.



Instrument noise spectral density



Paik-21



Electrostatic patch fields



- Electrostatic patch fields and trapped magnetic flux limited the performance of GP-B superconducting gyros.
- Parasitic stiffness due to patch fields: $\frac{\partial F}{\partial x} \cong 1.8 \frac{\varepsilon_0 A v^2}{d^3}$ (Speake, 96)

Paik-22



Electrostatic patch fields



- Electrostatic patch fields and trapped magnetic flux limited the performance of GP-B superconducting gyros.
- Parasitic stiffness due to patch fields: $\frac{\partial F}{\partial x} \cong 1.8 \frac{\epsilon_0 A v^2}{d^3}$ (Speake, 96)
- For high-purity Nb, $v = 0.36$ V. With design parameters $A = 4$ cm² and $d = 0.2$ mm, the patch fields affect the spring constant of the SGG as

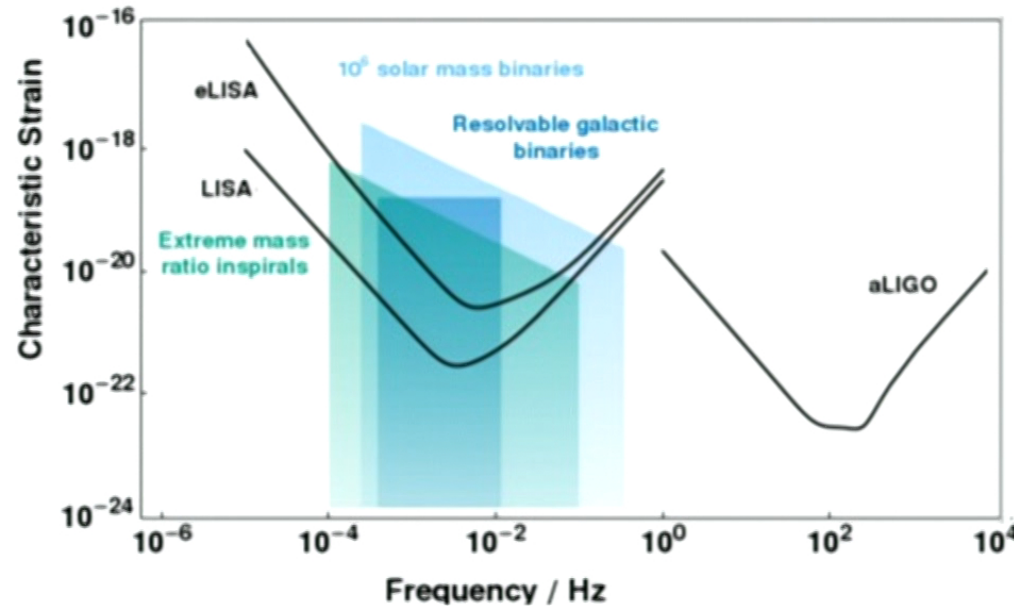
$$k = m \omega_c^2 - \frac{\partial F}{\partial x} = \left(1.58 - 1.0 \times 10^{-4} \right) \text{N/m}$$

- In high vacuum and temperature controlled environment, the patch fields should remain stationary in time.
- Parasitic stiffness due to patch fields (and trapped flux) modifies the CM stiffness only by one part in 10⁴ and is nulled in the process of axis alignment and CM balance (10⁹).

Paik-22



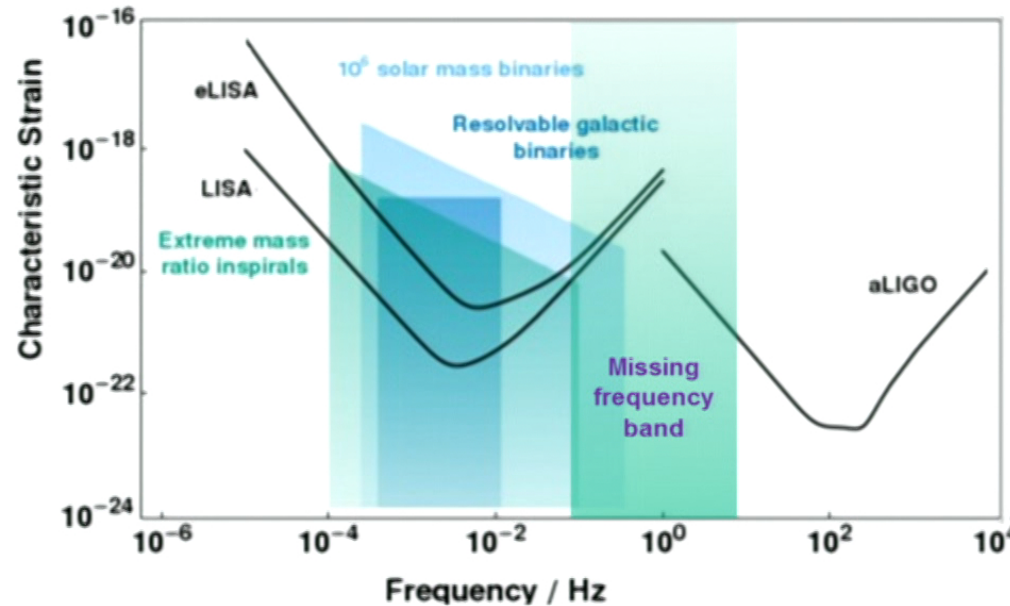
GW detector bandwidths



Paik-23



GW detector bandwidths



- Merger of IMBHs and inspiraling stellar mass BHs are expected to produce signals at 0.1 to 10 Hz bandwidth.
- Could a **terrestrial antenna** be built to fill this missing band?

Paik-23



Long-baseline resonant-mass detector



PHYSICAL REVIEW D

VOLUME 19, NUMBER 8

15 APRIL 1979

Tunable “free-mass” gravitational-wave detector

Robert V. Wagoner, Clifford M. Will, and Ho Jung Paik*

Institute of Theoretical Physics and Department of Physics, Stanford University, Stanford, California 94305

(Received 10 July 1978)

We propose a new type of detector for gravitational radiation. It consists essentially of two masses whose relative motion produces the driving emf of a resonant L - C circuit. The relative momentum of the masses induced by a gravitational wave is determined by the current in the circuit. A unique feature of this system is its ability to be tuned over a wide frequency range. If a quality factor $Q \sim 10^8$ can be achieved in the circuit, a laboratory-size detector cooled to 0.05 K in the absence of other noise could detect a continuous wave metric perturbation $h \gtrsim 3 \times 10^{-26}$ at the frequency of the Crab pulsar after integration for 100 days.

Paik-24



Long-baseline resonant-mass detector



PHYSICAL REVIEW D

VOLUME 19, NUMBER 8

15 APRIL 1979

Tunable “free-mass” gravitational-wave detector

Robert V. Wagoner, Clifford M. Will, and Ho Jung Paik*

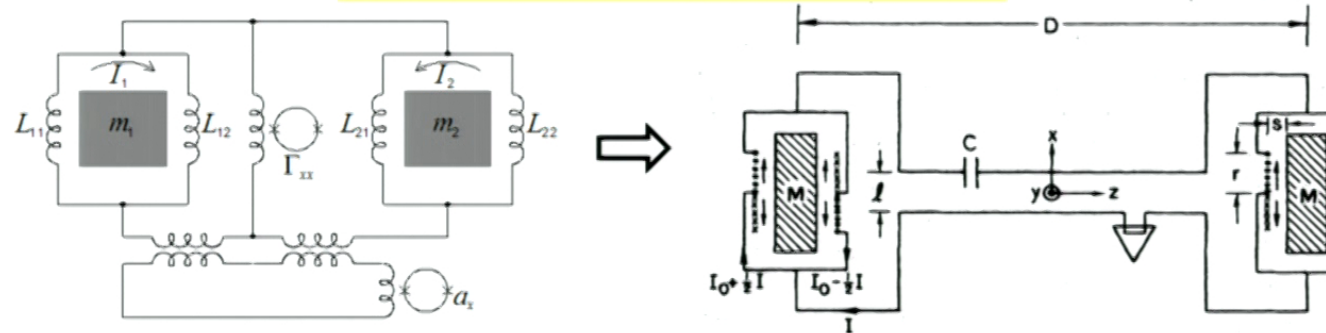
Institute of Theoretical Physics and Department of Physics, Stanford University, Stanford, California 94305

(Received 10 July 1978)

We propose a new type of detector for gravitational radiation. It consists essentially of two masses whose relative motion produces the driving emf of a resonant L - C circuit. The relative momentum of the masses induced by a gravitational wave is determined by the current in the circuit. A unique feature of this system is its ability to be tuned over a wide frequency range. If a quality factor $Q \sim 10^8$ can be achieved in the circuit, a laboratory-size detector cooled to 0.05 K in the absence of other noise could detect a continuous wave metric perturbation $h \gtrsim 3 \times 10^{-26}$ at the frequency of the Crab pulsar after integration for 100 days.

- Gravity gradients are Riemann tensor components.

$$R_{0i0j} \rightarrow \Gamma_{ij} = -\partial^2 \phi / \partial x_i \partial x_j \text{ in Newtonian limit.}$$

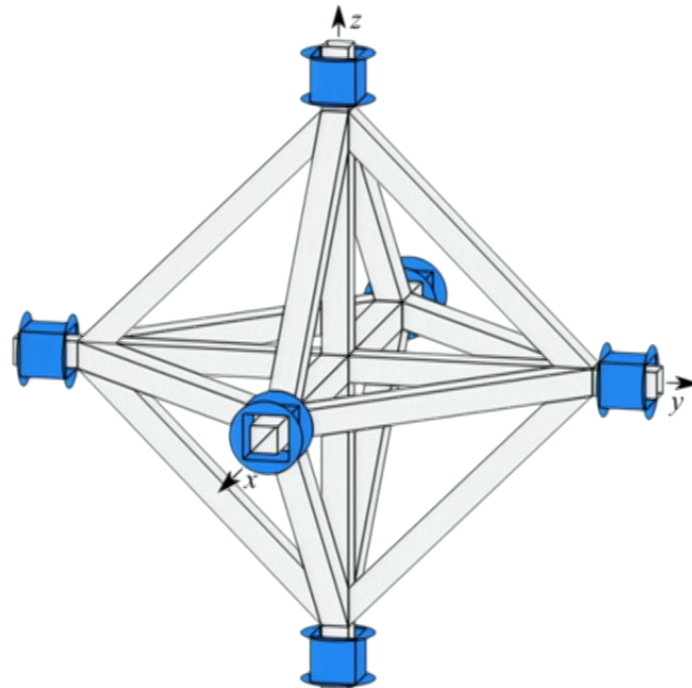




SOGRO (Superconducting Omni-directional Gravitational Radiation Observatory)



- Each test mass has **3 DOF**.
- Combining six test masses, **tensor** GW detector is formed.



$$h_{ii}(t) = \frac{2}{L} [x_{+ii}(t) - x_{-ii}(t)]$$

$$h_{ij}(t) = \frac{1}{L} \{ [x_{+ij}(t) - x_{-ij}(t)] - [x_{-ji}(t) - x_{+ji}(t)] \} \quad i \neq j$$

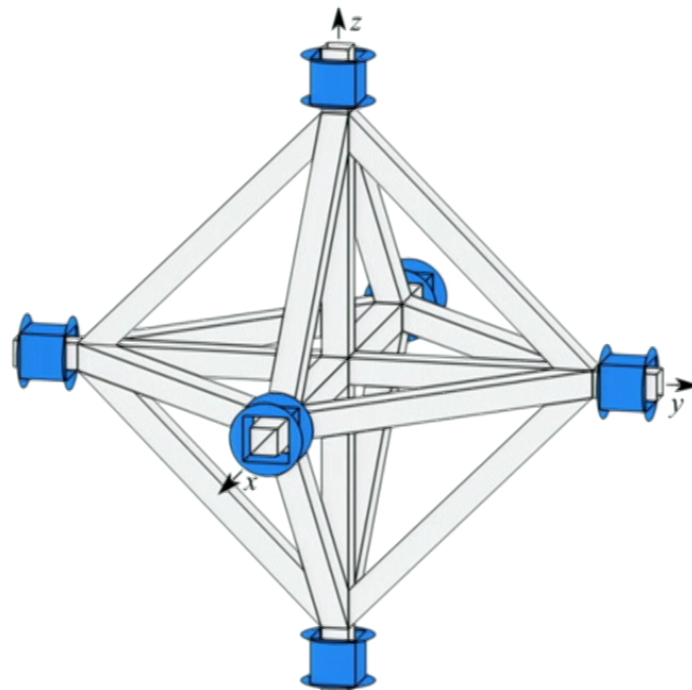
Paik-25



SOGRO (Superconducting Omni-directional Gravitational Radiation Observatory)



- Each test mass has **3 DOF**.
- Combining six test masses, **tensor** GW detector is formed.



$$h_{ii}(t) = \frac{2}{L} [x_{+ii}(t) - x_{-ii}(t)]$$

$$h_{ij}(t) = \frac{1}{L} \{ [x_{+ij}(t) - x_{-ij}(t)] - [x_{-ji}(t) - x_{+ji}(t)] \} \quad i \neq j$$

- Source direction (θ, ϕ) and polarization ($h+, h\times$) can be determined by a **single** antenna. \Rightarrow "Spherical" Antenna



+ polarization



x polarization

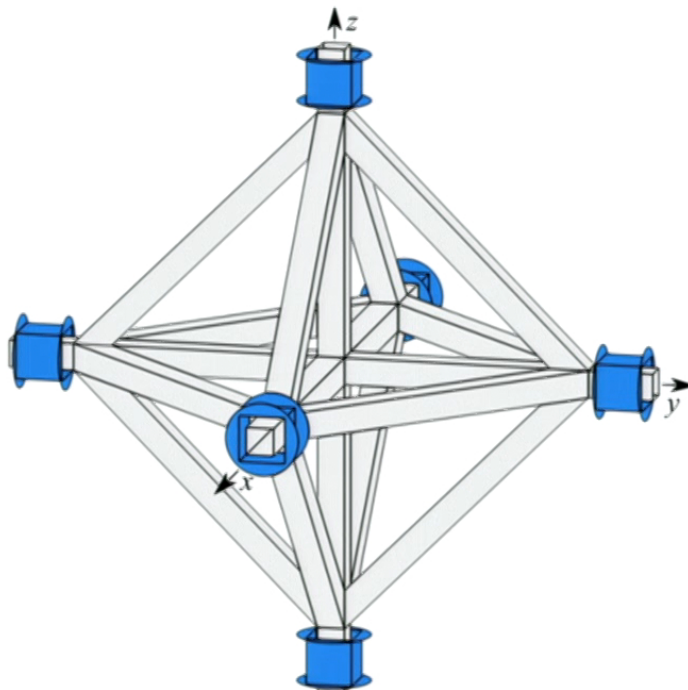
Paik-25



SOGRO (Superconducting Omni-directional Gravitational Radiation Observatory)



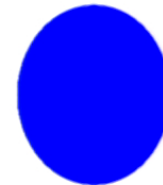
- Each test mass has **3 DOF**.
- Combining six test masses, **tensor** GW detector is formed.



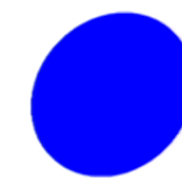
$$h_{ii}(t) = \frac{2}{L} [x_{+ii}(t) - x_{-ii}(t)]$$

$$h_{ij}(t) = \frac{1}{L} \{ [x_{+ij}(t) - x_{-ij}(t)] - [x_{-ji}(t) - x_{+ji}(t)] \} \quad i \neq j$$

- Source direction (θ, ϕ) and polarization ($h+, h\times$) can be determined by a **single** antenna. \Rightarrow "Spherical" Antenna



+ polarization



x polarization

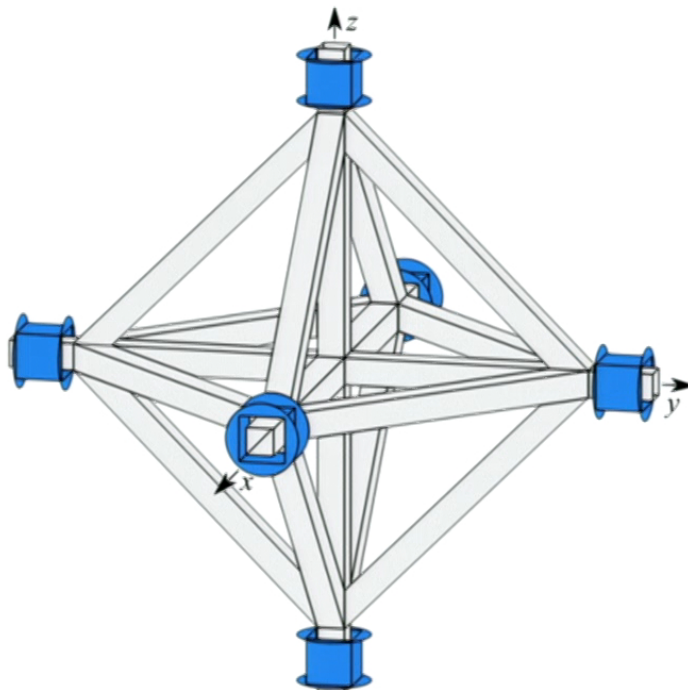
Paik-25



SOGRO (Superconducting Omni-directional Gravitational Radiation Observatory)



- Each test mass has **3 DOF**.
- Combining six test masses, **tensor** GW detector is formed.



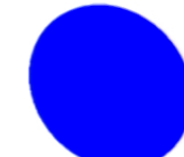
$$h_{ii}(t) = \frac{2}{L} [x_{+ii}(t) - x_{-ii}(t)]$$

$$h_{ij}(t) = \frac{1}{L} \{ [x_{+ij}(t) - x_{-ij}(t)] - [x_{-ji}(t) - x_{+ji}(t)] \} \quad i \neq j$$

- Source direction (θ, ϕ) and polarization ($h+, h\times$) can be determined by a **single** antenna. \Rightarrow "Spherical" Antenna



+ polarization



x polarization

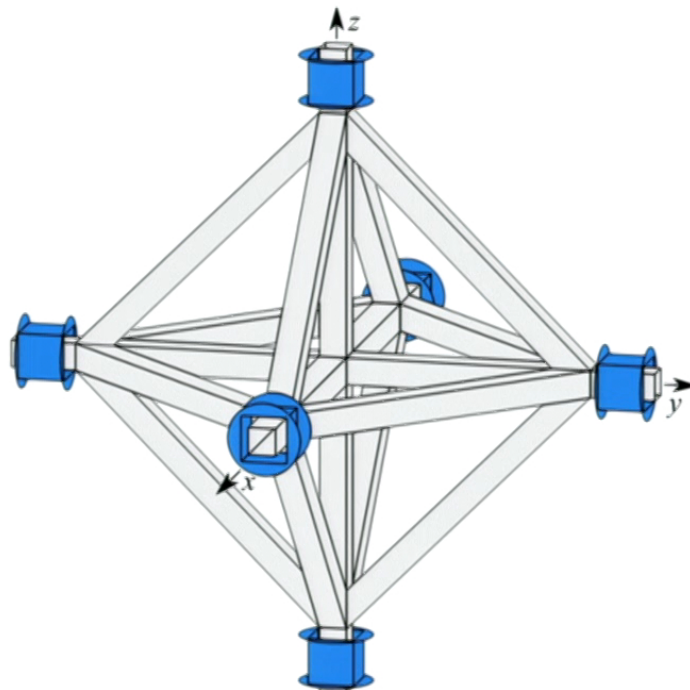
Paik-25



SOGRO (Superconducting Omni-directional Gravitational Radiation Observatory)



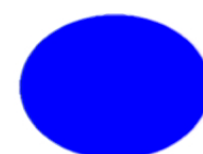
- Each test mass has **3 DOF**.
- Combining six test masses, **tensor** GW detector is formed.



$$h_{ii}(t) = \frac{2}{L} [x_{+ii}(t) - x_{-ii}(t)]$$

$$h_{ij}(t) = \frac{1}{L} \{ [x_{+ij}(t) - x_{-ij}(t)] - [x_{-ji}(t) - x_{+ji}(t)] \} \quad i \neq j$$

- Source direction (θ, ϕ) and polarization ($h+, h\times$) can be determined by a **single** antenna. \Rightarrow "Spherical" Antenna



+ polarization



x polarization

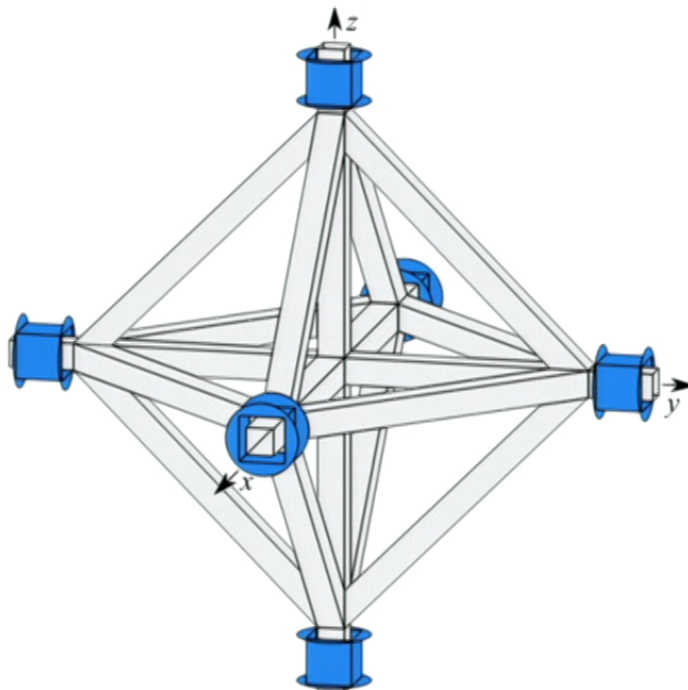
Paik-25



SOGRO (Superconducting Omni-directional Gravitational Radiation Observatory)



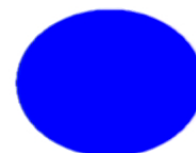
- Each test mass has **3 DOF**.
- Combining six test masses, **tensor** GW detector is formed.



$$h_{ii}(t) = \frac{2}{L} [x_{+ii}(t) - x_{-ii}(t)]$$

$$h_{ij}(t) = \frac{1}{L} \{ [x_{+ij}(t) - x_{-ij}(t)] - [x_{-ji}(t) - x_{+ji}(t)] \} \quad i \neq j$$

- Source direction (θ, ϕ) and polarization ($h+, h\times$) can be determined by a **single** antenna. \Rightarrow "Spherical" Antenna



+ polarization



x polarization

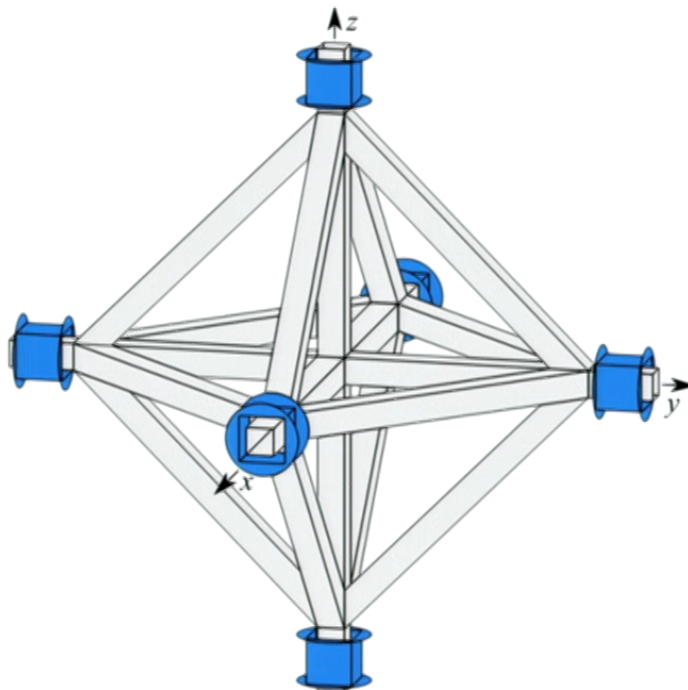
Paik-25



SOGRO (Superconducting Omni-directional Gravitational Radiation Observatory)



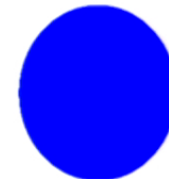
- Each test mass has **3 DOF**.
- Combining six test masses, **tensor** GW detector is formed.



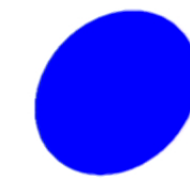
$$h_{ii}(t) = \frac{2}{L} [x_{+ii}(t) - x_{-ii}(t)]$$

$$h_{ij}(t) = \frac{1}{L} \{ [x_{+ij}(t) - x_{-ij}(t)] - [x_{-ji}(t) - x_{+ji}(t)] \} \quad i \neq j$$

- Source direction (θ, ϕ) and polarization ($h+, h\times$) can be determined by a **single** antenna. \Rightarrow "Spherical" Antenna



+ polarization



x polarization

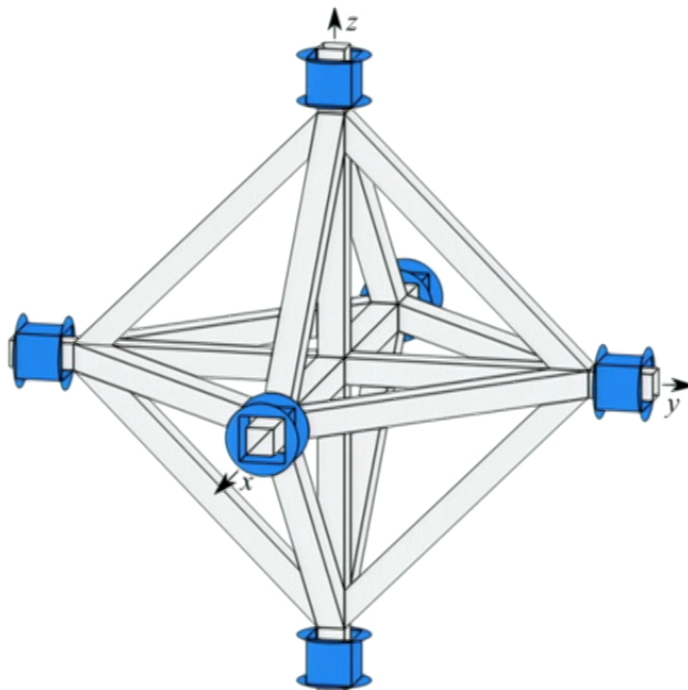
Paik-25



SOGRO (Superconducting Omni-directional Gravitational Radiation Observatory)



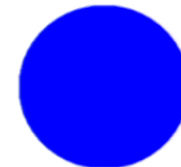
- Each test mass has **3 DOF**.
- Combining six test masses, **tensor** GW detector is formed.



$$h_{ii}(t) = \frac{2}{L} [x_{+ii}(t) - x_{-ii}(t)]$$

$$h_{ij}(t) = \frac{1}{L} \{ [x_{+ij}(t) - x_{-ij}(t)] - [x_{-ji}(t) - x_{+ji}(t)] \} \quad i \neq j$$

- Source direction (θ, ϕ) and polarization ($h+, h\times$) can be determined by a **single** antenna. \Rightarrow "Spherical" Antenna



+ polarization



x polarization

Paik-25

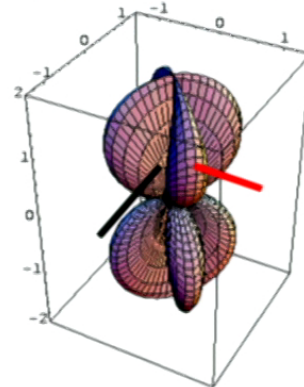


Antenna pattern

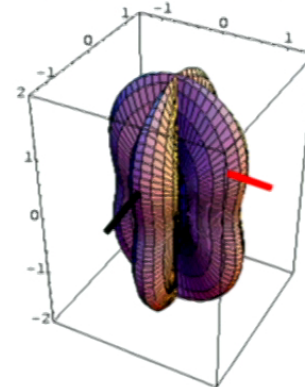


LIGO

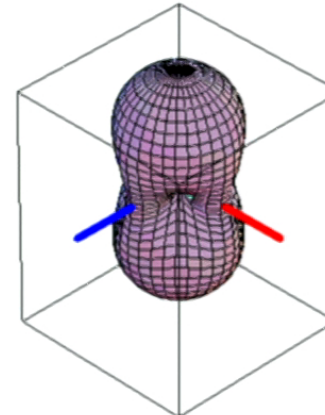
x polarization



+ polarization



rms sensitivity



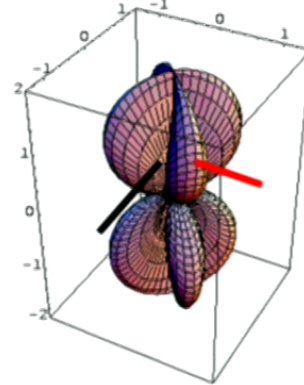


Antenna pattern

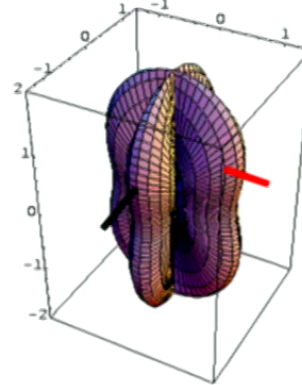


LIGO

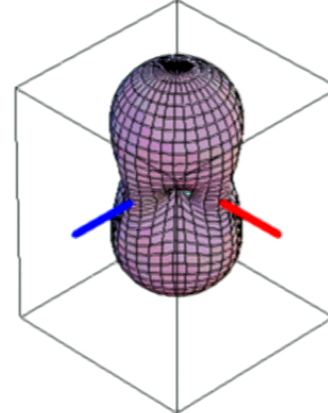
x polarization



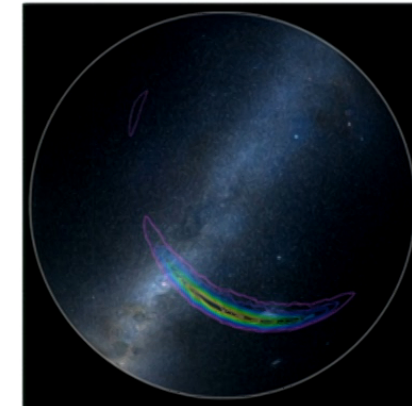
+ polarization



rms sensitivity



Sky location of GW150914





Design philosophy of SOGRO



$$\ddot{h}_{ij} = 2\Gamma_{ij} \rightarrow h_{GW}(f) > h_N(f) = \frac{2}{\omega^2} \Gamma_N(f)$$

As f is lowered from 100 Hz to 1 Hz, $\Gamma_N(f)$ must be lowered by 10^4 for the same $h_{GW}(f)$.

- Extremely low detector noise is required.
 ⇒ *Low T, high Q, nearly quantum-limited* amplifier.
- Test mass suspension frequency should be lowered to below signal bandwidth.
 ⇒ *Almost free* test masses by magnetic levitation.
- Seismic noise is very difficult to isolate at low frequencies.
 ⇒ High *CM rejection* in a superconducting differential accelerometer.
- Newtonian noise increases sharply below 10 Hz and *cannot* be shielded.
 ⇒ *Tensor* detector can help mitigate the NN.

H. J. Paik, C. E. Griggs, M. V. Moody, K. Venkateswara, H. M. Lee, A. B. Nielsen, E. Majorana and J. Harms, *Class. Quantum Grav.* **33**, 075003 (2016)

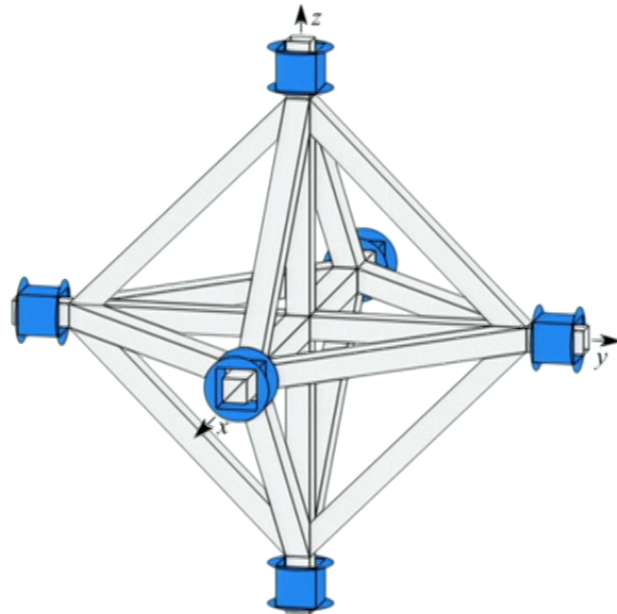
Paik-27



Suspension of SOGRO platform



- Go underground (> 500 m) to reduce the seismic and Newtonian noise, as well as to be far away from moving objects.
- Infrasound is attenuated to 0.15 at 0.2 Hz and to 10^{-8} at 1 Hz.
 - Platform needs to be rigid with all DM modes > 10 Hz and $Q > 10^6$.
➡ Careful engineering design required.



Paik-28

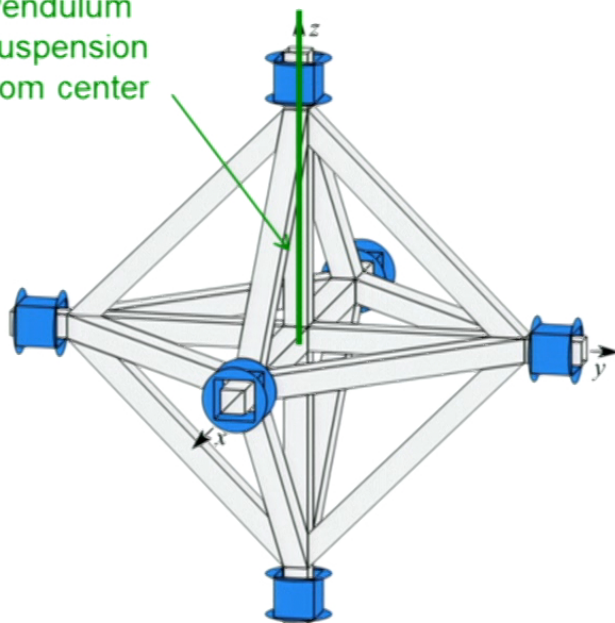


Suspension of SOGRO platform



- Go underground (> 500 m) to reduce the seismic and Newtonian noise, as well as to be far away from moving objects.
- Infrasound is attenuated to 0.15 at 0.2 Hz and to 10^{-8} at 1 Hz.

Pendulum suspension from center



- Platform needs to be rigid with all DM modes > 10 Hz and $Q > 10^6$.
⇒ Careful engineering design required.
- Nodal support prevents odd harmonics from being excited.
- 50-m pendulum: $f_p = 0.07$ Hz for pendulum modes and $f_\phi < 10^{-2}$ Hz for torsional mode.
⇒ Completely decouples ground tilt and provides > 40 dB isolation at 1 Hz for horizontal and torsional modes.

Paik-28

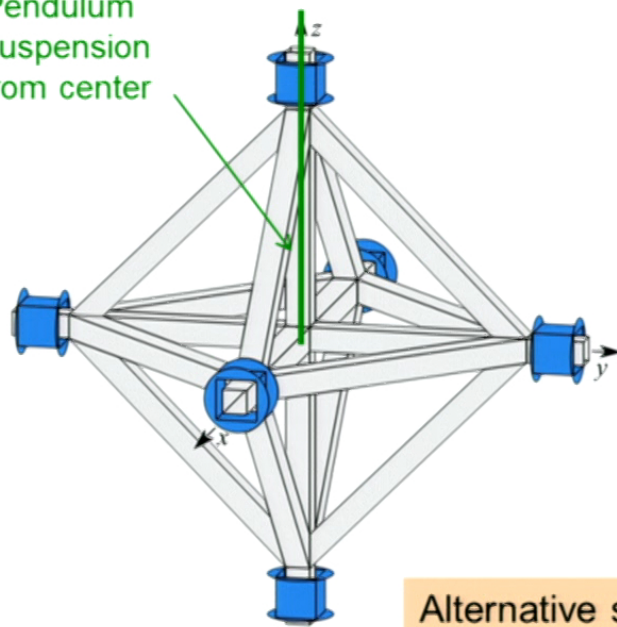


Suspension of SOGRO platform



- Go underground (> 500 m) to reduce the seismic and Newtonian noise, as well as to be far away from moving objects.
- Infrasound is attenuated to 0.15 at 0.2 Hz and to 10^{-8} at 1 Hz.

Pendulum suspension from center



- Platform needs to be rigid with all DM modes > 10 Hz and $Q > 10^6$.
⇒ Careful engineering design required.
- Nodal support prevents odd harmonics from being excited.
- 50-m pendulum: $f_p = 0.07$ Hz for pendulum modes and $f_\phi < 10^{-2}$ Hz for torsional mode.
⇒ Completely decouples ground tilt and provides > 40 dB isolation at 1 Hz for horizontal and torsional modes.

Alternative suspension: Optical rigid body
Simpler cryogenics, larger baseline (≥ 1 km?)

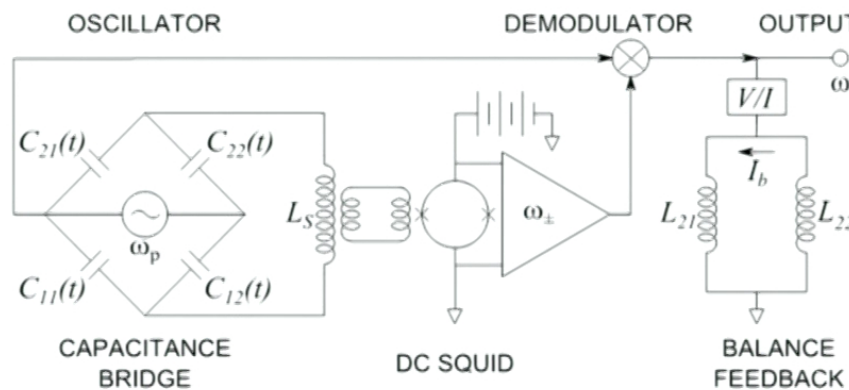
Paik-28



Tuned capacitor-bridge transducer



- Near quantum-limited SQUIDs have **1/f noise** below 10 kHz.
- Signal needs to be **upconverted** to ≥ 10 kHz by using an **active transducer**.
- **Capacitor bridge** coupled to **nearly quantum-limited SQUID**.



Cinquegrana et al., PRD 48, 448 (1993)

- Bridge is driven at LC resonance frequency ω_p .

- **Energy coupling:**

$$\beta \approx \frac{2CE_p^2Q_p}{M|\omega^2 - \omega_D^2|} > 1$$

- **Oscillator noise is rejected** by the bridge balance.

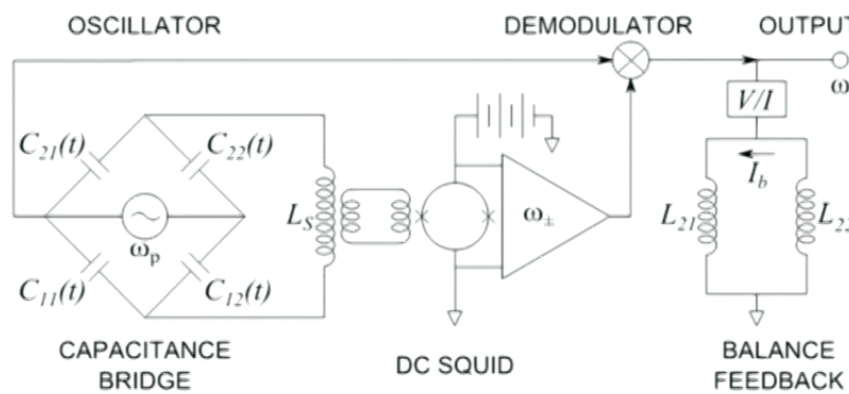
Paik-29



Tuned capacitor-bridge transducer



- Near quantum-limited SQUIDs have **1/f noise** below 10 kHz.
- Signal needs to be **upconverted** to ≥ 10 kHz by using an **active transducer**.
- **Capacitor bridge** coupled to **nearly quantum-limited SQUID**.



Cinquegrana et al., PRD 48, 448 (1993)

- Bridge is driven at LC resonance frequency ω_p .
- **Energy coupling:**

$$\beta \approx \frac{2CE_p^2Q_p}{M|\omega^2 - \omega_D^2|} > 1$$

- **Oscillator noise is rejected** by the bridge balance.

$$S_h(f) = \frac{16}{ML^2\omega^4} \left\{ \frac{k_B T \omega_D}{Q_D} + \frac{|\omega^2 - \omega_D^2|}{2\omega_p} \left(1 + \frac{1}{\beta^2} \right)^{1/2} k_B T_N \right\}, \quad k_B T_N = n\hbar\omega_p$$

Paik-29



Astrophysics with SOGRO



Parameter	SOGRO	aSOGRO
Each test mass M	5 ton	5 ton
Arm-length L	50 m	50 m
Antenna temp T	4.2 K	0.1 K
Platform temp T_{pl}	4.2 K	4.2 K
DM frequency f_D	0.01 Hz	0.01 Hz
DM Q factor Q_D	10^7	10^8
Platform Q factor Q_{pl}	10^6	10^7
Pump frequency f_p	50 kHz	50 kHz
Amplifier noise no. n	20	5
Detector noise $S_h^{1/2}(f)$	$3 \times 10^{-20} \text{ Hz}^{-1/2}$	$5 \times 10^{-21} \text{ Hz}^{-1/2}$

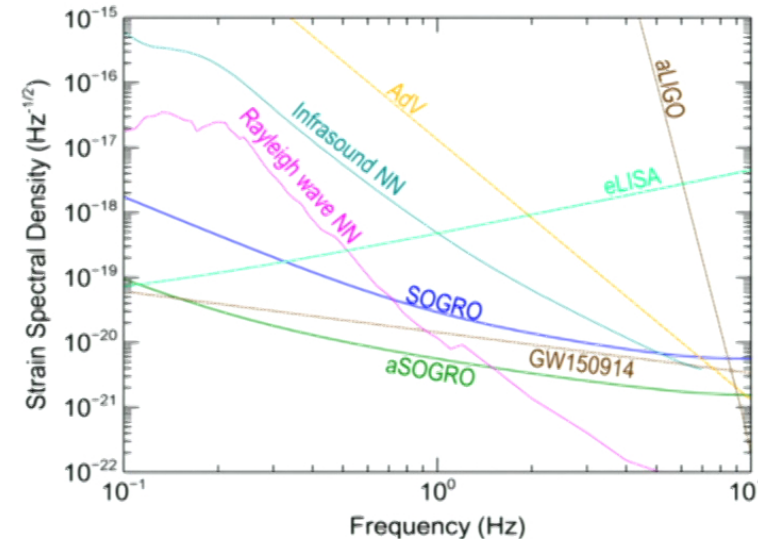
Paik-30



Astrophysics with SOGRO



Parameter	SOGRO	aSOGRO
Each test mass M	5 ton	5 ton
Arm-length L	50 m	50 m
Antenna temp T	4.2 K	0.1 K
Platform temp T_{pl}	4.2 K	4.2 K
DM frequency f_D	0.01 Hz	0.01 Hz
DM Q factor Q_D	10^7	10^8
Platform Q factor Q_{pl}	10^6	10^7
Pump frequency f_p	50 kHz	50 kHz
Amplifier noise no. n	20	5
Detector noise $S_h^{1/2}(f)$	$3 \times 10^{-20} \text{ Hz}^{-1/2}$	$5 \times 10^{-21} \text{ Hz}^{-1/2}$



- aSOGRO could detect **IMBH binaries** with $10^4\text{-}10^5 M_\odot$ at a few billion light years away, and **WD binaries** within the Local Group.
- aSOGRO could detect **BH binaries** like **GW150914** with SNR ~ 5 .
⇒ Alert interferometers days before merger.

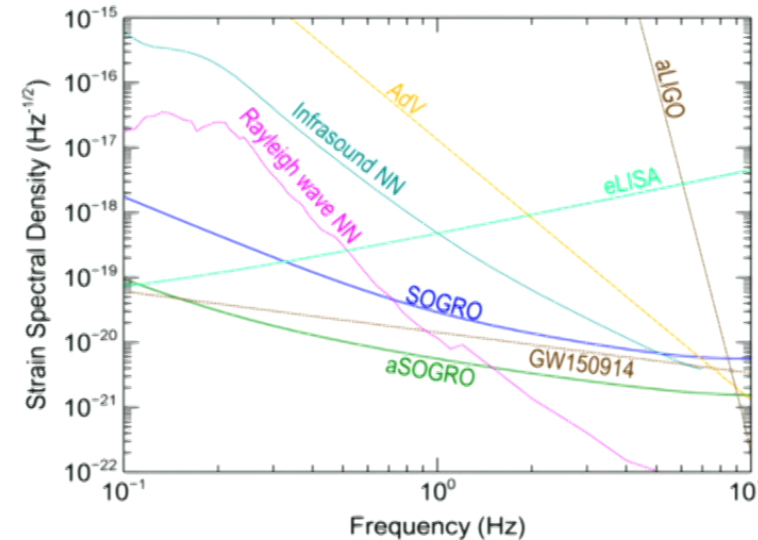
Paik-30



Astrophysics with SOGRO



Parameter	SOGRO	aSOGRO
Each test mass M	5 ton	5 ton
Arm-length L	50 m	50 m
Antenna temp T	4.2 K	0.1 K
Platform temp T_{pl}	4.2 K	4.2 K
DM frequency f_D	0.01 Hz	0.01 Hz
DM Q factor Q_D	10^7	10^8
Platform Q factor Q_{pl}	10^6	10^7
Pump frequency f_p	50 kHz	50 kHz
Amplifier noise no. n	20	5
Detector noise $S_h^{1/2}(f)$	$3 \times 10^{-20} \text{ Hz}^{-1/2}$	$5 \times 10^{-21} \text{ Hz}^{-1/2}$



- aSOGRO could detect **IMBH binaries** with $10^4\text{-}10^5 M_\odot$ at a few billion light years away, and **WD binaries** within the Local Group.
- aSOGRO could detect **BH binaries** like **GW150914** with SNR ~ 5 .
⇒ Alert interferometers days before merger.

SOGRO is being studied by a consortium of research institutions in Korea.

Paik-30



Electrostatic patch fields



- Electrostatic patch fields and trapped magnetic flux limited the performance of GP-B superconducting gyros.
- Parasitic stiffness due to patch fields: $\frac{\partial F}{\partial x} \cong 1.8 \frac{\varepsilon_0 A v^2}{d^3}$ (Speake, 96)
- For high-purity Nb, $v = 0.36$ V. With design parameters $A = 4$ cm² and $d = 0.2$ mm, the patch fields affect the spring constant of the SGG as

$$k = m \omega_c^2 - \frac{\partial F}{\partial x} = \left(1.58 - 1.0 \times 10^{-4} \right) \text{N/m}$$

- In high vacuum and temperature controlled environment, the patch fields should remain stationary in time.
- Parasitic stiffness due to patch fields (and trapped flux) modifies the CM stiffness only by one part in 10⁴ and is nulled in the process of axis alignment and CM balance (10⁹).